Time-Dependent Quark-Antiquark Potential and Quarkonia Suppression in Heavy-Ion Collisions

By

Partha Bagchi

PHYS07200904006

Institute of Physics, Bhubaneswar

A thesis submitted to the

Board of Studies in Physical Sciences

In partial fulfillment of requirements

For the Degree of

DOCTOR OF PHILOSOPHY

of

HOMI BHABHA NATIONAL INSTITUTE

December, 2015

STATEMENT BY AUTHOR

This dissertation has been submitted in partial fulfillment of requirements for an advanced degree at Homi Bhabha National Institute (HBNI) and is deposited in the Library to be made available to borrowers under rules of the HBNI. Brief quotations from this dissertation are allowable without special permission, provided that accurate acknowledgement of source is made. Requests for permission for extended quotation from or reproduction of this manuscript in whole or in part may be granted by the Competent Authority of HBNI when in his or her judgment the proposed use of the material is in the interests of scholarship. In all other instances, however, permission must be obtained from the author.

Date:- 23^{rd} December 2015 (Partha Bagchi)

CERTIFICATE

This is to certify that the thesis entitled "**Time-Dependent Quark-Antiquark Potential and Quarkonia Suppression in Heavy-Ion Collisions**", which is being submitted by **Mr. Partha Bagchi**, in partial fulfillment of the degree of **Doctor of Philosophy in Physics** of **Homi Bhabha National Institute** is a record of his own research work carried by him. He has carried out his investigations for the last six years on the subject matter of the thesis under my supervision at **Institute of Physics, Bhubaneswar**. To the best of our knowledge, the matter embodied in this thesis has not been submitted for the award of any other degree.

Signature of the Candidate **Signature of the Supervisor**

Partha Bagchi
Institute of Physics
Bhubaneswar

Dr. Ajit M. Srivastava
Professor
Institute of Physics
Bhubaneswar

Date:- 23^{rd} December 2015.

DECLARATION

I, Partha Bagchi, hereby declare that the investigations presented in the thesis have been carried out by me. The matter embodied in the thesis is original and has not been submitted earlier as a whole or in part for a degree/diploma at this or any other Institution/University.

Date: 23^{rd} December 2015 (Partha Bagchi)

To My Family

Contents

Acknowledgement

I am deeply thankful to my thesis supervisor Prof. Ajit Mohan Srivastava for giving me the meaning of the term PHILOSOPHY that comes in PhD. He is not only a good physicist, he is an excellent human being. I am grateful to him that he accepted me as his student. I have learnt physics as well as the meaning of life from him whatever I know. From the inception of my PhD carrier he became such a friend that with whom I discussed my personal problems also. It is better to stop now, otherwise I would write pages about him.

This is my opportunity to thank my family. I am thankful to my parents for giving me everything they can. What I am right now, only because of them. Especially, many thanks to my sister, because of her I am here. She stood with me when I refused to go for a school teaching job during my MSc. I want to thank my Dida (Late grand mother) who used to call me doctor, but not in the sense, hopefully I will become. Also I want to thank my beloved wife Sreya for giving me support and love. I think I am very much fortunate to have such a family like this.

I want to thank Prof. Somendra Mohan Bhattacharjee, Prof. Sudipta Mukherjee, Prof. Avinash Khare and prof. Ajit Mohan Srivastava (My supervisor) for excellent teaching during one year course work in IOP, Bhubaneswar. I also want to thank Prof. Kalyan Kundu and Sikha Verma for creating friendly and positive academic atmosphere in IOP. I want to thank Dr. Chinmoy Basu, Dr. Arunabha Bhadra, Dr. Gurupada Chaudhuri, Dr. Dhruba Dasgupta, Sri Rajat Kr. Dey, Dr. Swapan Kr. Ghosal, Dr Ashok Ghosh, Sri. Ashok Guha, Dr. Sakuntala Gupta and Dr. Amitabha Mukhopadhyay during my BSc. and MSc. days who motivated me for research. Specially I want to thank Sri. Anupam Bhoumik, who first influenced me to continue with physics. May be he does not know that if he would have not taught me physics then I would have chosen mathematics rather than physics.

Now among friends in my batch I would first take the name of Rama who supported me in every moments during my PhD life. May be because of him I continued my PhD at IOP. Also I want to thank Tanmoy, Sabita and Shubhashis who always supported me during my IOP life. I enjoyed attending classes with all my batchmates Indrani, Rama, Sabita, Shubhashis and Tanmoy.

Among my IOP and NISER colleagues, I want to thank Souvik da with whom I

discussed not only physics, but also many personal problems. Also I want to thank Ambresh da, Trilochan da, Sachin da, Ajay da, Chitrasen da, Sanjib da, Subhasis da, Sabya, Bidisha, Priyo, Surasree, Chirashree, Pratik, Arnab, Anjan for various physics discussions. I enjoyed small self cooked dinner party with Souvik da, Ranjita di, Shubhashis, Arnab, Sabya, Tanmoy, Rama, Sarita, Surasree, Chirashree and Bidisha. Specially I liked Biriyani by Sabya, Mutton by Shubhashis, Paneer by Rama and almost all the dishes made by Surasree and Chirashree. Some of the dishes, mainly Khichidi, I learnt from Souvik da. Also I enjoyed playing several games with Bipul da, Vanraj, Raghavendra, Tanmoy, Rama, Tanmoy, Shubhashis, Arnab, Anjan, Puspendu, Priyo, Shreyansh, Chandan, Arpan and Debasis. I want to thank all of them for making my IOP life memorable.

Now I want to thank all my group members Sanatan da, Rajarshi da, Soma di, Biswanath da, Ananta da, Ranjita di, Saumia di, Abhishek da, Arpan, Shreyansh, Nirupam and Somnath da. Discussing with them was always enjoyable. I will never forget those discussions with Abhishek da when we missed our lunch because of discussion. Specially I want to thank Arpan, Shreyansh and Somnath da who checked many chapters of my thesis.

Again I want to thank all of them who made this duration of my PhD tenure memorable.

Date: 23^{rd} December 2015 **Partha Bagchi**

Synopsis

Relativistic heavy ion collision experiments (e.g. at RHIC, LHC) provide us the opportunity to produce the deconfined phase of quantum chromo dynamics (QCD), known as quark gluon plasma (QGP). QGP also existed in the early Universe, when the universe was a few microsecond old. Relativistic heavy ion collisions, where QGP phase is produced for a very short time is the only lab experiment where the condition similar to early Universe can be produced.

QCD, the theory of strong interaction is an $SU(3)$ gauge theory. Here gauge charges are color charges. Two most important prediction of QCD are asymptotic freedom and confinement. The strong interaction coupling constant is given by,

$$\alpha_s\left(Q^2\right) = \frac{4\pi}{(11 - 2n_f/3)\ln\left(Q^2/\Lambda^2\right)} \tag{0.1}$$

where $\Lambda \sim 200\ MeV$ is known as the QCD scale, n_f is the number of flavors in the theory and Q^2 is the momentum transfer . Since $n_f = 6$, the coupling decreases with the increase in the momentum transfer. At very high energy or large momentum transfer α_s asymptotically approaches zero and the interaction between quarks and gluons becomes very weak so they can move almost freely. This phenomena is known as asymptotic freedom [1, 2]. Other phenomena confinement comes from the fact that experimentally we have never observed any colored particle as an isolated physical state. Experimentally we have observed mesons and baryons which are color singlet. Attractive interaction between a quark and an antiquark has a confining part (apart from the Coulombic part) which increases with the separation between Quark-Antiquark. This makes it impossible to separate a single quark or antiquark from a hadron. This phenomena is known as quark confinement or in general as color confinement.

QCD predicts that under suitable physical condition there should be a phase transition between confined and deconfined matter. At extreme conditions of very high energy density and/or baryon density, hadrons undergo a phase transition to a deconfined phase, where quarks and gluons forget the identity of the hadron to which they belong, and they can travel freely across a distance which is larger than typical hadron size. Phase transitions are characterized by some order parameter, which takes different values in different phases. For QCD, thermal expectation of Polyakov loop

$l(x)$ [3] acts as an order parameter for confinement deconfinemnt phase transition.

$$l(x) = \mathrm{Tr}\left\{ \mathbf{P}\left[\exp\left(ig \int_0^\beta d\tau A_0(x) \right) \right] \right\}. \tag{0.2}$$

where, $A_0(\vec{x},\tau) = A_0^a(\vec{x},\tau)T^a, (a = 1, \ldots N)$ are the gauge fields and T^a are the generators of $SU(N)$ in the fundamental representation. For QCD $N = 3$. $\mathbf{P}$ denotes the path ordering in the Euclidean time τ, $\beta = T^{-1}$(T is the temperature) and g is the gauge coupling. $l(x)$ is related to free energy of a test quark, $\langle l(x)\rangle = e^{-\beta\Delta F}$. In confined phase free energy becomes infinite and order parameter vanishes and in deconfined phase free energy becomes finite and $l(x)$ also becomes finite. As the QCD Lagrangian is invariant under any arbitrary $SU(3)$ transformation, using the periodicity of gauge field in euclidean time direction one can show that allowed transformation for l is $l(x) \longrightarrow z \times l(x)$. Here z is the element of $Z(3) \in SU(3)$, with $z = e^{i\phi}$ and $\phi = 0, 2\pi/3, 4\pi/3$. As in confined phase l vanishes, it respect $Z(3)$ symmetry, whereas in the deconfined phase it takes finite value and $Z(3)$ symmetry breaks spontaneously. This leads to 3 degenerate vacua corresponding to $l = 1, e^{2\pi i/3}, e^{4\pi i/3}$. After symmetry breaking the order parameter field can choose any of the three vacua, hence domains with different l will be produced. The junction of different domains gives rise to topological defects, known as $Z(3)$ domain walls. We have calculated the profile of these walls ($l(x)$ profile) between different vacua. Using the effective potential (at finite temperature) of Polyakov loop given by Pisarski [4], we have numerically extracted $l(x)$ profile by minimizing the energy [5]. We then extract the profile of gauge field A_0 associated with the $Z(3)$ domain wall profile by inverting the above equation for $l(x)$. Using the $l(x)$ profile and using diagonal gauge choice for A_0, we have self consistently obtained the A_0 profile [6]. It has been shown earlier that this A_0 profile associated with a $Z(3)$ wall has CP violating effects [7–9]. This means on interaction with the background field, quarks and antiquarks scatters differently.

There have been various signals proposed for the detection of QGP in relativistic heavy-ion collisions. Though there is no single unique signal which allows a straightforward identification of the quark-gluon plasma phase. However, strong evidence from several signals has been accumulating in support of the presence of the deconfined phase of matter in heavy-ion collisions. Quarkonia suppression is one such signature of QGP. Matsui and Satz [10] first proposed J/ψ suppression as a signature

of QGP. The conventional mechanism for quarkonia suppression is such that due to the presence of QGP medium, potential between $q\bar{q}$ is Debye screened, resulting in the swelling of quarkonia. If the Debye screening length of the medium is less than the radius of quarkonia, then $q\bar{q}$ may not form bound states. Due to this melting, the yield of quarkonia will be *suppressed*. In conventional mechanism if the temperature (T) remains at certain value (T_D) where Debye length is larger than the size of quarkonia, then there will be no melting of quarkonia. Here we have discuss that even the temperature remain below T_D, the quarkonia will melt in medium.

In first case we have shown that the CP violating effects of background gauge field associated with $Z(3)$ walls can lead to disintegration of quarkonia. We consider the quarkonia moving through the wall. As the interaction is CP violating, the quark and antiquark of the system will be pulled apart from each other, this lead to spatial excitation of the system. As the background gauge field A_0 associated with the wall carries color, the interaction also changes color composition of the system. We start with color singlet J/ψ and consider the gauge field (A_0 profile) as perturbation and calculate the transition to an octet χ state. Using first order perturbation theory we show that the transition probability rapidly increases with velocity or kinetic energy of incoming quarkonia. As the octet states are not bound, they will melt in the medium. Hence, yield of J/ψ will be suppressed [11].

There are certain conceptual issues in this scenario due to use of the CP violating gauge field associated with the profile of $l(x)$. Thus it becomes important to study whether heavy quarkonia disintegration due to the $Z(3)$ domain walls essentially requires such CP violating interaction. We consider the interaction of q and $\bar{q}$ as in [5] where the interaction is modeled in terms of an effective quark mass which depends on the magnitude of $l(x)$. Again using the space dependent mass as perturbation and using first order perturbation theory we found that quarkonia on interaction with $Z(3)$ walls has non-zero probability of getting excited to higher states which are short lived in the medium. This is happening because the perturbation acts on different space time points for the quark and the antiquark in the system. As there is no color charge associated with $l(x)$ or $m(x)$, we have only spatial excitation. In this case the transition probability first increases with velocity and attains a maximum value and again decreases. This behavior is a distinguishable feature of our model, which is not

present in the conventional mechanism of quarkonia suppression.

In next work, we question the validity of the assumption of adiabatic evolution of quarkonia states during thermalization which underlies the conventional mechanism based on Debye screening. We show that during thermalization stage quarkonia can get excited because of the time dependence of the potential between quark and antiquark. In conventional mechanism the basic picture assumes that when potential changes then quarkonia wave function modifies itself adiabatically. One then investigates whether such a quarkonium state is bound or not, depending on the Debye screening. This assumption of adiabatic evolution requires that the time scale for change in potential be large enough compared to the typical time scale associated with the dynamics of the system, e.g. the time scale associated with energy gap between the successive energy states. At very high energy it is likely that thermalization is achieved in a very short time of order 0.25 fm for RHIC and 0.1 fm for LHC [12]. Also elliptic flow data shows that thermalization achieves within 1 fm [13]. This time scale is comparable to the time scale associated with energy gap. Thus the validity of adiabatic evolution does not hold. The problem thus needs to be treated using time dependent perturbation theory and one should calculate the survival probability of quarkonia under this perturbation. Considering the thermalization time scale to be small enough (from various estimates and elliptic flow data) we have used sudden approximation. We found that even when temperature of QGP remains below T_D, the quarkonium state decays with significant probability [14]. Survival probability decreases with temperature of the medium. Also we have found that the probability drops very significantly near T_D. We have also estimated the error in using first order perturbation theory which is the probability that the initial quarkonium state does not remain in the same state during the time period τ (taken as 0.5 fm here) of the change of the potential. This probability remains below 8 % for the thermalization time used $\leq$ 1 fm. This shows the validity of approximation of first order perturbation theory for our calculations.

In conclusion, we have proposed alternative mechanisms of quarkonia suppression in relativistic heavy-ion collisions which do not require temperature to necessarily exceed the Debye temperature of the quarkonium state under consideration. Our mechanisms have distinctive features which can be used to distinguish them from the

conventional mechanism of quarkonia suppression.

Bibliography

[1] D. J. Gross and F. Wilczek, Phys. Rev. Lett. **30**, 1343 (1973).

[2] H. D. Politzer, Phys. Rev. Lett. **30**, 1346 (1973).

[3] A. M. Polyakov, Phys. Lett. B **72**, 477 (1978).

[4] R. D. Pisarski, Phys. Rev. D **62**, 111501 (2000) [hep-ph/0006205].

[5] B. Layek, A. P. Mishra, A. M. Srivastava and V. K. Tiwari, Phys. Rev. D **73**, 103514 (2006) [hep-ph/0512367].

[6] A. Atreya, A. M. Srivastava and A. Sarkar, Phys. Rev. D **85**, 014009 (2012) [arXiv:1111.3027 [hep-ph]].

[7] C. P. Korthals Altes and N. J. Watson, Phys. Rev. Lett. **75**, 2799 (1995) [hep-ph/9411304].

[8] C. P. Korthals Altes, K. M. Lee and R. D. Pisarski, Phys. Rev. Lett. **73**, 1754 (1994) [hep-ph/9406264].

[9] C. P. Korthals Altes, In *Dallas 1992, Proceedings, High energy physics, vol. 2* 1443-1447

[10] T. Matsui and H. Satz, Phys. Lett. B **178**, 416 (1986).

[11] A. Atreya, P. Bagchi and A. M. Srivastava, Phys. Rev. C **90**, no. 3, 034912 (2014) [arXiv:1404.5697 [hep-ph]].

[12] D. M. Elliott and D. H. Rischke, Nucl. Phys. A **671**, 583 (2000) [nucl-th/9908004].

[13] P. F. Kolb and U. W. Heinz, Published in *Hwa, R.C. (ed.) et al.: Quark gluon plasma* 634-714 [nucl-th/0305084].

[14] P. Bagchi and A. M. Srivastava, Mod. Phys. Lett. A **30**, 32, 1550162 (2015) [arXiv:1411.5596 [hep-ph]].

List of Publications

1. **Published**

   (a) *****_A Novel Mechanism for J/ψ Disintegration in Relativistic Heavy Ion Collisions_
   Abhishek Atreya, **Partha Bagchi**, Ajit M. Srivastava
   Phys. Rev. C90 (2014) 3 034912; arXiv:1404.5697 [hep-ph];

   (b) *****_Quarkonia Disintegration due to time dependence of the $q\bar{q}$ potential in Relativistic Heavy Ion Collisions_
   Partha Bagchi, Ajit M. Srivastava
   Mod. Phys. Lett. A 30, 32, 1550162 (2015); arXiv:1411.5596

   (c) _Spontaneous CP Violating Quark Scattering From Asymmetric $Z(3)$ Interfaces in QGP_
   Abhishek Atreya, **Partha Bagchi**, Arpan Das, Ajit M. Srivastava
   Phys. Rev. D90 (2014) 12, 125016; arXiv:1406.7411;

   (d) _Effects of phase transition induced density fluctuations on pulsar dynamics_
   Partha Bagchi, Arpan Das, Biswanath Layek, Ajit M. Srivastava
   Phys. Lett. B747 (2015) 120-124; arXiv:1506.03287

   (e) _Probing Non-Standard Interactions at Daya Bay_
   Sanjib Kumar Agarwalla, **Partha Bagchi**, David V. Forero, Mariam Tortola
   JHEP 1507 (2015) 060; arXiv:1412.1064

   (f) _Reaction-diffusion equation for quark-hadron transition in heavy-ion collisions_
   Partha Bagchi, Arpan Das, Srikumar Sengupta, Ajit M. Srivastava
   Phys. Rev. C92 (2015) 3, 034902; arXiv:1507.01015

(*****) indicates the papers on which this thesis is based.

2. **In arxiv**

   (a) *Probing Dynamics of Phase Transitions occurring inside a Pulsar*
   Partha Bagchi, Arpan Das, Biswanath Layek, Ajit M. Srivastava
   arXiv:1412.4279

   (b) *Possibility of DCC formation in pp collisions at LHC energy via reaction-diffusion equation*
   Partha Bagchi, Arpan Das, Srikumar Sengupta, Ajit M. Srivastava
   arXiv:1508.07752

3. **Conference Proceedings**

   (a) *A Novel Mechanism for J/ψ Disintegration in Relativistic Heavy Ion Collisions*
   Abhishek Atreya, **Partha Bagchi**, Ajit M. Srivastava
   Proc. Indian Natl. Sci. Acad. 81 (2015) 207-212

   (b) *Disintegration of quarkonia in QGP due to time dependent potential*
   Partha Bagchi, Ajit M. Srivastava
   PoS CPOD2014 (2015) 050.

4. **Manuscript Under Preparation**

   (a) *****_Disintegration of quarkonia in Heavy Ion Collisions due to non-trivial profile of the Polyakov loop of $Z(3)$ interfaces_
   Abhishek Atreya,**Partha Bagchi**, Ajit M. Srivastava

(*****) indicates the papers on which this thesis is based.

List of Figures

Chapter 1

Introduction

1.1 Journey From Molecule to Quark

The thirst for going deep inside matter started a long ago when molecule was proposed as the smallest constituents of pure chemical substances. Then, chronologically, John Dalton gave Atomic Theory, J. J. Thomson (1897) discovered electron, Rutherford proposed substructure of atom as electron and heavy mass nucleus in 1911, then he discovered proton ($1917 - 1919$, named by him, 1920), James Chadwick discovered neutron in 1932. Subsequently, quark was discovered as elementary constituent of matter [1, 2]. This is clearly not the end, the search is still going on.

In the next two section we will discuss very briefly about Quantum Chromo Dynamics (QCD), the theory of strong interaction. We will also discuss different phases and the phase diagram of QCD.

1.2 QCD, The Theory of Strong Interaction

In this section we will primarily follow references [3–5]. The quarks and gluons interact with each other via strong interaction. The theory of strong interaction is QCD where quarks and gluons are the fundamental particles which carry color charge. QCD is a non-abelian gauge theory with gauge group SU(3). Quarks transform under fundamental representation of $SU(3)$ and carry three types of color charge, named as red, blue and green, while antiquarks carry anti-color charges. The interaction

between quarks are mediated by gauge bosons, called gluons. There are 8 types of gluons in QCD. They transformed as adjoint representation of $SU(3)$. The Lagrangian for QCD is written as,

$$\mathcal{L} = -\frac{1}{4} G^a_{\alpha\beta} G^{\alpha\beta}_a + \bar{\psi} \left(i\gamma^\mu D_\mu - m \right) \psi, \tag{1.1}$$

where D_μ is called the covariant derivative and is given by,

$$D_\mu = \partial_\mu - igT_a A^a_\mu. \tag{1.2}$$

where T_a are the generators of $SU(3)$ in the fundamental representation. They satisfies the commutation relation

$$[T^a, T^b] = f^{abc} T^c. \tag{1.3}$$

Here f^{abc} are the structure constants. $G_{\alpha\beta}$ is the gluonic field strength tensor, which is related to the commutator of covariant derivative as,

$$\Big[D_\alpha, D_\beta \Big] = igG_{\alpha\beta} \equiv igT_a G^a_{\alpha\beta}, \tag{1.4a}$$

$$\text{where} \quad G^a_{\alpha\beta} = \partial_\alpha A^a_\beta - \partial_\beta A^a_\alpha + g f^{abc} A^b_\alpha A^c_\beta. \tag{1.4b}$$

The transformation of fields under $SU(3)$ transformation U are given by

$$\psi \to \psi' = U\psi, \tag{1.5a}$$

$$\text{and} \quad T_a A^a_\mu \to T_a A^a_\mu{}' = U T_a A^a_\mu U^{-1} - i\Big(\partial_\mu U \Big) U^{-1}. \tag{1.5b}$$

From the QCD Lagrangian one can easily see that there are self-interaction terms for gluons like,

$$g\partial_\nu A^a_\mu f^{abc} A^{\mu b} A^{\mu c} \quad \text{and} \quad g^2 f^{abc} f^{alm} A^b_\mu A^c_\nu A^{\mu l} A^{\mu m}.$$

The corresponding Feynman diagrams have three point and four point vertices for gauge bosons. This is a generic feature of every gauge theory (like QCD) with a non-abelian gauge group that gauge fields have self interactions. Thus gluons carries charge and self interact, unlike photons which are gauge bosons of an abelian gauge theory with U(1) gauge group. This can also be seen directly by constructing Noether charge for the gluon field.

One of the most important features of QCD is asymptotic freedom, that follows from running coupling constant of QCD

$$\alpha_s\left(Q^2\right) = \frac{4\pi}{(11 - 2n_f/3)\ln\left(Q^2/\Lambda^2\right)}, \tag{1.6}$$

where $\Lambda \sim 200\ MeV$ is known as the QCD scale and n_f is the number of flavors in the theory. Since $n_f = 6$, the coupling decreases with the increase in the momentum transfer Q^2. So at very large momentum transfer, the coupling constant approaches to very small value. This phenomenon is known as asymptotic freedom of QCD [6, 7]. Hence, at very high energy and/or small distances (thus high density) the quarks and gluons should move freely. The above expression also shows that for low energy, coupling constant becomes very high, that means the interaction becomes stronger at large distance.

1.3 Color Confinement

Quarks and gluons are not observed experimentally as isolated particles. They are bound into hadrons, namely, mesons which are quark-antiquarks bound states, and baryons which are bound states of three quarks. As gluons self-interact, one also expects bound states consisting only of gluons, named as glueballs. However so far there is no clear experimental evidence of these objects. Absence of isolated quarks and gluons is related to another remarkable property of QCD, that the the color force between a quark and antiquark inside a hadron is not only Coulomb like, there is a confining part which increases with distance. This confining part comes from multi gluon exchange between quarks. This makes impossible to remove a quark from a hadron. This phenomena is known as color confinement. There is no theoretical proof for this yet (apart from lattice gauge theory). In this case the perturbative treatment, based on an expansion in powers of the coupling constant, is not valid. So to explain confinement a non-perturbative treatment is needed.

1.3.1 Bag Model of Confinement

A phenomenological model which is very useful for studying non perturbative quark-gluon system is M.I.T. bag model [8]. This takes into account both the asymptotic freedom and color confinement. In this model a hadron has an internal structure associated with quarks and the gluon fields which are taken to be localized in a spatial region. This region is called a bag. Quarks are treated as massless particles inside a bag of finite dimension, and are infinitely massive outside the bag. The kinetic energy of quarks constitutes a pressure, pushing the bag outward which is balanced by a bag pressure (B) which tries to pull them inward. Hence, in this model, finite size hadron results from the balance between two pressures. The phenomenological quantity, B, is introduced to take into account the non-perturbative color confining aspect of QCD. The total color charge of the matter inside the bag must be colorless, by virtue of the Gauss's Law. With three different types of color, the only allowable hadronic bags are colorless qqq and $q\bar{q}$ states. Glueballs are incorporated in this model by considering gluonic fields confined inside the bag.

The simple picture can be used to estimate the bag pressure. With that one can see how at extreme conditions of very high temperature and/or baryon density one expects liberation of color charges leading to the formation of quark-gluon plasma (QGP). For this we will primarily follow ref. [9],

1.3.2 Hadrons and the bag pressure

Consider massless fermions in a spherical cavity of radius R. The Dirac equation for the fermions in that cavity is

$$\gamma.p\psi = 0 \tag{1.7}$$

In Dirac's representation

$$\gamma^0 = \begin{pmatrix} I & 0 \\ 0 & -I \end{pmatrix}$$

and

$$\gamma^i = \begin{pmatrix} 0 & \sigma^i \\ -\sigma^i & 0 \end{pmatrix}$$

Where I is 2×2 unit matrix and σ^i are Pauli matrices. The wave function ψ is written as

$$\psi = \begin{pmatrix} \psi_+ \\ \psi_- \end{pmatrix}$$

where ψ_+ and ψ_- are $2-d$ Dirac spinors. So Eq. 1.7 becomes,

$$\begin{pmatrix} P_0 & -\vec{\sigma}.\vec{P} \\ +\vec{\sigma}.\vec{P} & -P_0 \end{pmatrix} \begin{pmatrix} \psi_+ \\ \psi_- \end{pmatrix} = 0$$

After solving the above equation we'll have the ground state solution

$$\psi(\vec{r},t) = \begin{pmatrix} \psi_+(\vec{r},t) \\ \psi_-(\vec{r},t) \end{pmatrix} = \begin{pmatrix} Ae^{-ip_0 t} j_0(p^0 r)\chi_+ \\ Ae^{-ip_0 t}(\vec{\sigma}.\vec{r}) j_1(p^0 r)\chi_+ \end{pmatrix}$$

where j_0 & j_1 are spherical Bessel functions, $\chi_\pm$ are Dirac spinors and A is normalization constant.

The confinement of quarks only requires that vector current $j^\mu = \bar{\psi}\gamma^\mu\psi$ should vanish outside the cavity, that means the normal component of j^μ should be zero at the surface of the bag which is taken to be at $r = R$. This implies, for a normal vector n directing outward, $n_\mu j^\mu = \bar{\psi} n_\mu \gamma^\mu \psi = 0$. Since in the instantaneous rest frame, n_0 is zero and $\vec{n}$ is the ordinary unit vector normal to the surface of the cavity, it can be shown that $-i\gamma_\mu n^\mu \psi = \psi$. Hence $\bar{\psi}\psi = 0$ This gives

$$j_0(P^0 R) = j_1(P^0 R). \tag{1.8}$$

This has a solution

$$P^0 R = 2.04 \quad \text{or} \quad P^0 = \frac{2.04}{R}. \tag{1.9}$$

So the kinetic energy of a quark inside a bag is inversely proportional to the radius of the bag. (This is expected also from simple application of uncertainty principle). Consider a system of N quarks inside a bag. Then the total energy of the system will be,

$$E = \frac{2.04N}{R} + \frac{4}{3}\pi R^3 B. \tag{1.10}$$

Where the last term comes from the contribution of the bag pressure. Equilibrium radius can be found by minimizing total energy, leading to

$$B^{\frac{1}{4}} = \left(\frac{2.04N}{4\pi}\right)^{\frac{1}{4}} \frac{1}{R}. \tag{1.11}$$

Assuming the radius of a three 3 quark hadron (baryon) to be 0.8 fm, from Eq. 1.11 one can calculate $B^{\frac{1}{4}} = 206\ MeV$

For more detail discussion of bag model see reference [10]

1.4 Deconfinement in QCD and quark-gluon plasma

As we mentioned above, at very high energies and very short distances, quarks and gluons are expected to move freely due to asymptotic freedom of QCD. This leads to the expectation that at very high temperatures (with very high thermal kinetic energies of quarks and gluons) and/or very high baryon densities (implying very short distances), one should get a gas of weakly interacting quarks and gluons where color charges are no more confined within hadronic length scales. Such a system of quarks and gluons with liberation of color charges is called the quark-gluon plasma.

Perturbative calculation for deconfined phase of QCD give satisfactory results [11], but most of those are in high temperature limit. For the values of temperatures near the transition temperature, only reliable calculations are from lattice at zero baryon chemical potential. There are few perturbative calculation for finite baryon density also. Lattice calculations also have been performed for finite baryonic chemical potential, though different techniques give varying estimates for the critical point etc. Here we will discuss the matter at extreme conditions in the Bag model.

As we discussed, in the bag model hadrons are confined inside a bag which has a definite finite size due to balance between bag pressure and the pressure resulting from the particles inside the bag. If the parton number is increased inside the bag, as will happen at high temperature T, it will lead to increase in outward pressure. Similarly, an increase in the density or baryon chemical potential μ_B will be expected to increase the pressure due to larger Fermi momentum of partons. Hence one expects that there will be a critical value of T and/or μ_B above which the bag pressure can not hold the partons. As a result a new phase of matter containing quarks and gluons is possible in which liberated quarks and gluons are in thermal equilibrium. The phase is known as the deconfined phase of partonic mater or the Quark-Gluon Plasma. Using standard methods all the thermodynamic quantities can be calculated considering a noninteracting system of massless quarks and gluons. In this *ideal gas*

limit, resulting expressions for pressure P, entropy density S, energy density $\mathcal{E}$ and number density n. are as follows, [12],

$$P = \left(g_g + \frac{7}{8}g_f\right)\frac{\pi^2 T^4}{90} + \frac{g_f}{24}\left(\mu_q^2 T^2 + \frac{\mu_q^4}{2\pi^2}\right) \tag{1.12a}$$

$$\mathsf{S} = 2\left(g_g + \frac{7}{8}g_f\right)\frac{\pi^2 T^3}{45} + \frac{g_f}{12}\mu_q^2 T \tag{1.12b}$$

$$\mathcal{E} = \left(g_g + \frac{7}{8}g_f\right)\frac{\pi^2 T^4}{30} + \frac{g_f}{8}\left(\mu_q^2 T^2 + \frac{\mu_q^4}{2\pi^2}\right) \tag{1.12c}$$

$$n = \frac{g_f}{12}\left(\mu_q T^2 + \frac{\mu_q^3}{\pi^2}\right). \tag{1.12d}$$

Where g_g is degeneracy factor for gluons and g_f is degeneracy factor for fermions. $\mu_q = 3\mu_B$ is the quark chemical potential. We will consider two flavor degrees of freedom, which is reasonable approximation up to RHIC energy, and we will discuss the behavior of plasma in the two extreme regimes, at high temperature and at high density.

1.4.1 Quark Gluon Plasma at High Temperature

For this we will take the case of zero baryon density, i.e. $\mu_B = 0$. Thus, the pressure in this case is given by (Eq. 1.12a),

$$P = 37\frac{\pi^2}{90}T^4 \tag{1.13}$$

The critical temperature T_c is the temperature above which this pressure exceeds the bag pressure B and the partons become deconfined. We get,

$$T_c = \left(\frac{90B}{37\pi^2}\right)^{\frac{1}{4}} \tag{1.14}$$

using the value $B^{\frac{1}{4}} = 206\ MeV$ we get $T_c \sim 144\ MeV$. Beyond this value of temperature the bag can't hold the matter inside it. Hence, quark matter is produced. Such a phase is believed to have existed in the early universe when the age of the universe less than few micro-seconds. During these stages the temperature was higher than the above value of T_c. Net baryon density was almost negligible in the universe so $\mu_B = 0$ is a good approximation .

1.4.2 Quark Gluon Plasma at High Density

Next extreme regime we consider is that at zero temperature and at high baryon density. The pressure can be found from Eq. 1.12a,

$$P = \frac{{\mu_q}^4}{2\pi^2}. \tag{1.15}$$

Again for the critical value of quark chemical potential μ_c^q, this pressure is equal to the bag pressure B. Using $B^{\frac{1}{4}} = 206\ MeV$ one can get $\mu_c^q \sim 434\ MeV$ leading to the critical baryon number density $n_c \sim 0.72/fm^3$. The baryon number density (from nucleons) in normal nuclear matter is $\sim 0.16/fm^3$. So the critical baryon density is about 5 times the normal nuclear baryon number density.

For finite temperature and finite chemical potential, the critical temperature and critical baryon chemical potential will be some where in between the values for the above two extreme cases. In the next section we will discuss the qualitative features of the resulting QCD phase diagram.

1.5 QCD Phase Diagram

The QCD phase diagram as a function of temperature (T) and baryon chemical potential μ_B is shown in Fig.1.1 [13]. It gives an overall idea of different phases of QCD, and associated phase transitions. The qualitative aspects of this phase diagram can be represented in terms of three different regions.

There are lot of available lattice simulation for the region with zero chemical potential and finite temperatures. For realistic values of quark masses, lattice calculations predicts that there are no genuine phase transitions at zero μ_B, so there should not be any phase boundaries in this direction. Calculations indicate a crossover from the hadronic phase to the quark-gluon plasma for realistic u, d and s quark masses [14,15]. The crossover temperature is likely to be in the range $150 - 180\ MeV$. The early universe was in this region and the experiment like RHIC and LHC also explore this regime of phase transition for very small μ_B

If we move along the μ_B direction for zero temperature, then there is possibility of rich phase structures. First nuclear matter appears near $\mu_B \sim 940\ MeV$ which

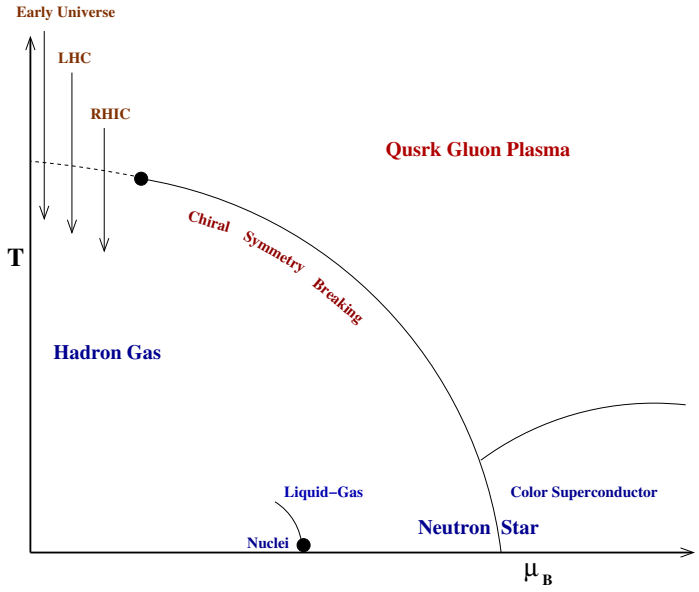

Figure 1.1: QCD phase diagram (see ref. [13]).

is separated from the hadronic gas by a first order transition line. For larger values of μ_B, neutron superfluidity is expected to occur (as inside neutron stars), where neutrons condense to form superfluid. As μ_B is further increased, high density QGP is expected to form. However, here several exotic phases are possible, such as color superconductor which results from condensation of quark Cooper pairs (which are formed due to attractive $q-q$ interaction in the 3^* channel) like electron-electron Cooper pair in normal superconductor. Detailed properties of such phases are not yet understood, for a review see ref. [16]. Other exotic phases are proposed in this high μ_B regime [13], like the Color Flavor Locked (CFL) phase, or the crystalline color superconductor. The core of neutron star may contain all these phases. The upcoming experiment compressed baryonic matter (CMB) at FAIR is expected to explore this region of high μ_B QCD.

For finite T and finite μ_B there are very few lattice calculations available. In this region effective field theory models predict first order phase transition. Combined with the lattice results which show a cross-over transition at low values of μ_B, we conclude that the first order transition line should end at a point with $T = T_c$ and $\mu_B = \mu_c$ at which the phase transition is second order. This point is the critical point in phase diagram. Several experiments are devoted to find this critical point.

There are many open question which remain to be answered about the QCD phase diagram. There are several experiment going on and several experiments are planed for the investigation of these aspects of QCD phase diagram.

The thesis is organized as follows: After this introduction, the next chapter (Chapter 2) contains a brief review of confinement-deconfinement phase transition and formation of topological defects like $Z(3)$ walls. It also contains numerical calculations for finding the profile of Polyakov loop order parameter $l(x)$ interpolating between two vacua as well as the profile of associated gauge field (A_0). The formation of QGP in laboratory and its signatures have been reviewed briefly in chapter 3. The time evolution of quantum states is discussed in chapter 4 in first order time-dependent perturbation theory. The two limits, adaibatic perturbation, and the sudden perturbation have been discussed in detail. Chapter 5 presents the new mechanism of quarkonia dissociation on interaction with the background gauge field associated with a $Z(3)$ wall. The interaction of $Z(3)$ walls with quarkonia and quarkonia dissociation by modeling effective mass as a function of $l(x)$ is presented in chapter 6. Quarkonia dissociation during thermalisation due to time dependenc of the quark-antiquark potential is discussed in chapter 7. Chapter 8 summarizes the work presented in this thesis.

Chapter 2

Confinement Deconfinement Phase Transition and Formation of Topological Defect

In this chapter, we will discuss the confinement-deconfinement phase transition as a spontaneous symmetry breaking phase transition, leading to topologically non-trivial vacuum manifold. This leads to topological structures such as domain walls and strings. We will start our discussion with topological defects and formation of topological defect with few example.

2.1 Topological Defects

When a symmetry is spontaneously broken, then it may imply existence of topological defects if the vacuum manifold has non-trivial topology. In condensed matter physics there are many examples of topological defects like string defects and point defects in liquid crystals, vortices in superfluid helium and flux tubes in superconductors. There are many example of topological defects in early universe, like cosmic strings, magnetic monopoles, and domain walls (for details, see [17]). In this section we will first discuss few examples of topological defects. Then we will discuss the process of formation of topological defects, usually known as the Kibble mechanism [18]. We will then discuss the formation of Z(3) domain walls which result from the spontaneous

breaking of $Z(3)$ symmetry in the confinement-deconfinement transition.

2.1.1 Examples of Topological Defects

The existence of different types of topological objects like domain walls, strings, monopole and textures depends on the topology of the vacuum. Here we will briefly discuss domain wall and string defects.

1. **Domain Walls :** Domain walls appear when a discrete symmetry is spontaneously broken leading to a disconnected vacuum manifold. Consider simple case of a single scalar field having double well potential after symmetry breaking. The Lagrangian can be written as,

$$L = \frac{1}{2}(\partial_\mu \phi)^2 - \frac{\lambda}{4}(\phi^2 - v^2)^2. \tag{2.1}$$

   The Lagrangian has discrete $Z(2)$ symmetry under the transformation $\phi \to -\phi$. The potential has two minima at $\phi = \pm v$. When the field chooses any of the vacua then the symmetry of ground state breaks spontaneously. If ϕ takes different vacuum values in any two different spatial regions then continuity of ϕ requires that these two regions are separated by a planar sheet where $\phi = 0$. This is the domain wall defect. 1-d Field equation has analytic solution, which gives the profile of this domain wall in physical space as shown in Fig. 2.1.

$$\phi = v \tanh(\sqrt{\frac{\lambda}{2}} vz). \tag{2.2}$$

   The solution ϕ passes through zero as it interpolates between the two different vacuum values from far left to far right.

2. **Strings :** String defects appear when a continuous symmetry breaks spontaneously leading to nontrivial first homotopy group of the vacuum manifold. If ϕ for the Lagrangian in Eq.2.1 is a complex scalar field then the Lagrangian has continuous U(1) symmetry with symmetry transformation $\phi \to e^{i\theta}\phi$. Where θ varies continuously from 0 to 2π. The potential in this case has a 'Mexican hat' shape with degenerate minima at $|\phi| = v$. A choice of vacuum with specific value of θ (say $\theta = 0$) breaks the U(1) symmetry spontaneously. String defect results when θ varies non-trivially in physical space as follows.

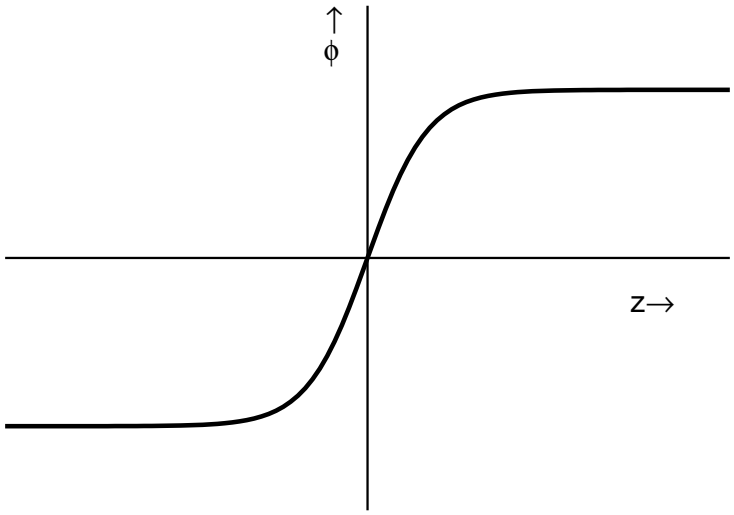

Figure 2.1: The domain wall configuration.

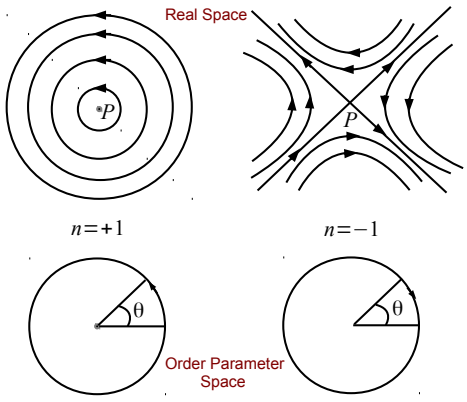

Figure 2.2: Field configuration for a vortex (string in 3 dimension)

When we traverse a closed path L in physical space it is possible for the field ϕ to wrap non-trivially around the circle of minima of the potential, so, the phase of ϕ develops a non-trivial winding. For example, net change in θ, $\Delta\theta = \pm 2\pi$ in Fig.2.2 ($+$ and $-$ signs correspond to the figures on left and right respectively). If we shrink the loop L in the physical space, we can locate the point where the field value has singularity and value is not defined . So the magnitude of the field will take zero value at that point. It is important to note that this *point* cannot be removed by any local change, we have to modify the full system to remove it. In 2-d, the location of this singularity represents a point defect which is a topological defect with unit winding. For $\Delta\theta = \pm 2\pi$ we get a defect and antidefect respectively. In three space dimensions, by shrinking the loop L in physical space at different (2-d) planes, one can easily see that the locus of this singularity represents a topological line or string defect.

2.1.2 Formation of Topological Defects: Kibble Mechanism

Kibble gave a general theory of formation of topological defects in a spontaneous symmetry breaking transition. He argued that after spontaneous symmetry breaking transition, domains of ordered phase form in physical space below Ginzberg temperature. The size of these domains will be of the order of correlation length at that temperature. The choice of order parameter in a domain is completely independent from the other one. In between the two domains, the order parameter varies following geodesic rule which states that the order parameter in between the two domains traces the shortest path on the vacuum manifold to minimize gradient energy term, present in the free energy.

If around the intersection of several of those domains, the order parameter has a topologically nontrivial variation, that means by local modification of the system this specific non-trivial variation cannot be removed, then the defect is called topological. The type of topological defect, like domain wall, string, monopole, or texture (topological object), depends on the topology of the vacuum and space dimensions.

2.2 Confinement-Deconfinement Phase Transition

In this section we will focus on confinement-deconfinement phase transition. First we will construct the order parameter for this transition, then from the symmetry considerations we will write the effective potential for the order parameter. In the entire discussion here we will consider pure QCD, where there are no dynamical quarks. We primarily follow the discussion in ref. [19].

2.2.1 Polyakov Loop Order Parameter

Consider $SU(N)$ gauge theory at finite temperature *without* dynamical quarks. Let us denote the states by $|s_G\rangle$. The partition function of the system is then written as

$$\mathcal{Z} = Tre^{-\beta F} = \sum_{s_G} \langle s_G | e^{-\beta H} | s_G \rangle. \tag{2.3}$$

In order to distinguish confined phase from the deconfined one, we will consider free energies of infinitely massive static quarks and antiquarks. Let us introduce operators, $\psi_a^\dagger(\vec{x_0}, t)$ and $\psi_a(\vec{x_0}, t)$ which create and annihilate static quarks with color a at position x_0, and time t, along with their charge conjugates for antiquarks. These field operators satisfy the anticommutation relations

$$\{\psi_a(\vec{x_1}, t), \psi_b^\dagger(\vec{x_2}, t)\} = \delta_{ab}\delta^3(\vec{x_1} - \vec{x_2}). \tag{2.4}$$

Similar relation holds also for conjugate fields, and all other equal-time anti-commutators vanishes. The (Euclidean) time evolution of the wave function is given by Dirac equation in the Euclidean space.

$$\left(-i\partial_0\delta^{ab} - gA_0^{ab}(\vec{x_0}, \tau)\right)\psi_b(\vec{x_0}, \tau) = 0, \tag{2.5}$$

where $A_0 = A_0^i\lambda_i$, with λ_i being the Gell-Mann matrices. This gives the solution as

$$\psi_a(\vec{x_0}, \beta) = \mathbf{P}\left[\exp\left(ig\int_0^{\tau=\beta} d\tau A_0(\vec{x_0}, \tau)\right)\right]_{ab}\psi_b(\vec{x_0}, 0), \tag{2.6}$$

where $\mathbf{P}$ denotes path ordering forward in time.

Now our aim is to find whether the system is in the confined phase or in the deconfined phase. For this purpose, we introduce an infinitely heavy test quark,

placed at position $\vec{x_0}$, as a probe. (As the test quark should not have any back reaction, that means the test quark should be static in medium, so we consider the test quark as infinitely heavy.) In the presence of this test quark the state of the system is given by $|s\rangle = \psi_a^\dagger(\vec{x_0}, 0)|s_G\rangle$. Hence the partition function becomes

$$\begin{aligned} \mathcal{Z}_q = e^{-\beta F(\vec{x_0})} &= \frac{1}{N}\sum_s \langle s|e^{-\beta H}|s\rangle \\ &= \frac{1}{N}\sum_{s_G}\langle s_G|\sum_a \psi_a(\vec{x_0},0)e^{-\beta H}\psi_a^\dagger(\vec{x_0},0)|s_G\rangle, \end{aligned} \tag{2.7}$$

where N is the number of colors. $N = 3$ for QCD. Thus the sum over a is on all possible color states. Now just like the operator e^{-iHt} generates the time translation in Minkowski time, $e^{-\beta H}$ generates the time translation in Euclidean space. Thus, in the Euclidean space, for any operator O,

$$e^{\beta H}O(t)e^{-\beta H} = O(t+\beta). \tag{2.8}$$

This implies

$$e^{\beta H}\psi_a(\vec{x_0},0)e^{-\beta H} = \psi_a(\vec{x_0},\beta), \tag{2.9a}$$

$$\Rightarrow \mathcal{Z}_q = \frac{1}{N}\sum_{s_G}\langle s_G|\sum_a e^{-\beta H}\psi_a(\vec{x_0},\beta)\psi_a^\dagger(\vec{x_0},0)|.s_G\rangle \tag{2.9b}$$

The time evolved field in Eq. 2.6 is related to the initial field by an overall phase. This overall phase is the non-Abelian analogue of Bohm-Arhanov phase and is called the Wilson line. In the Euclidean space, due to the periodicity in time direction, it becomes a loop. The trace of this quantity over all color degree of freedom is known as the Polyakov Loop. It is defined as

$$L(\vec{x}) = \frac{1}{N}\mathrm{Tr}\left\{\mathbf{P}\left[\exp\left(ig\int_0^{\tau=\beta} d\tau A_0(\vec{x_0},\tau)\right)\right]\right\}. \tag{2.10}$$

Using eq. (2.6) and eq. (2.10) in eq. (2.9), we get

$$\mathcal{Z}_q = \sum_{s_G}\langle s_G|e^{-\beta H}L(\vec{x})|s_G\rangle. \tag{2.11}$$

Dividing this by the partition function of the pure glue system, we get the change in the free energy of the system in the presence of the test quark as,

$$\frac{\mathcal{Z}_q}{\mathcal{Z}} \equiv e^{-\beta\Delta F} = \langle L(\vec{x})\rangle. \tag{2.12}$$

As we are dealing with static, infinitely massive quark, the free energy of a single quark system does not carry much sense. However, for a quark at positions $\vec{x}$ and an anti-quark at position $\vec{y}$, one can show the free energy of the system is function of the distance between the quark and the anti-quark as

$$\langle L^{\dagger}(\vec{y})L(\vec{x})\rangle \propto e^{-\beta F_{q\bar{q}}}. \tag{2.13}$$

- **For confining phase**, the free energy required to separate a quark from an anti quark is infinite. That means $F_{q\bar{q}} \to \infty$ as the separation between the quark and antiquark increases. Also if the quark and antiquarks are far away from each other, then one will expect Polyakov loops at these positions to be uncorrelated. Thus $\langle L^{\dagger}(\vec{y})L(\vec{x})\rangle \longrightarrow \langle L^{\dagger}(\vec{y})\rangle\langle L(\vec{x})\rangle = |\langle L(\vec{x})\rangle|^2$. Then Eq.(2.13) becomes

  $$|\langle L(\vec{x})\rangle|^2 \propto e^{-\beta F_{q\bar{q}}}. \tag{2.14}$$

  Hence $\langle L(x)\rangle = 0$ in the confining phase.

- **For deconfined phase**, $F_{q\bar{q}}$ is finite, hence $\langle L(x)\rangle$ is finite. One can normalized $\langle L(x)\rangle$ to unity

Thus Polyakov loop can be used to distinguish the confinement as an order parameter. It vanishes in the confined phase and becomes unity in the deconfined phase at high temperature.

2.2.2 Spontaneous Breaking of $Z(3)$ Symmetry and $Z(3)$ Domain Walls

We now discuss symmetry properties of the Polyakov loop order parameter. The QCD Lagrangian is invariant under any arbitrary $SU(3)$ transformation. Let us consider $U(x,\tau) \in SU(3)$ to be the transformation. Then the transformation of gauge fields and consequently that of Polyakov Loop are given as

$$A_{\mu}(x,\tau) \longrightarrow A'_{\mu}(x,\tau) = U(x,\tau)A_{\mu}(x,\tau)U(x,\tau)^{-1} + iU(x,\tau)\partial_{\mu}U(x,\tau)^{-1} \tag{2.15}$$

$$L(\vec{x}) \longrightarrow L(\vec{x})' = \frac{1}{N}\mathrm{Tr}\left\{U(x,\beta)\mathbf{P}\left[\exp\left(ig\int_0^{\tau=\beta} d\tau A_0(\vec{x_0},\tau)\right)\right]U(x,0)\right\} \tag{2.16}$$

Since the gauge fields are periodic in the direction of Euclidean time, only those transformation are allowed which preserve the periodic boundary conditions of the gauge fields. We note that with $A_\mu(x,0) = A_\mu(x,\beta)$, the relation $A'_\mu(x,\beta) = A'_\mu(x,0)$ holds from Eq. (2.15) if $U(x,\beta) = ZU(x,0)$, such that $Z \in SU(N)$, commutes with all the $SU(N)$ matrices and is space-time independent. Under this transformation Polyakov Loop also transform as

$$L(\vec{x}) \longrightarrow ZL(\vec{x}). \tag{2.17}$$

By definition, the set of all such elements Z, is called the center group of $SU(N)$ denoted by $Z(N)$. The elements of $Z(N)$ are

$$Z = e^{i\phi}\mathbf{1}; \quad \phi = 2\pi m/N; \quad m = 0, 1 \ldots (N-1) \tag{2.18}$$

For the case of QCD, $N = 3$. Thus we conclude that finite temperature pure QCD is invariant under Z(3) symmetry transformations. The Polyakov loop transforms according to eq. (2.17) under this $Z(3)$. Hence the order parameter $\langle L(\vec{x})\rangle \longrightarrow Z\langle L(\vec{x})\rangle$. In the confining phase $\langle L(\vec{x})\rangle = 0$ which implies $\langle L(\vec{x})\rangle$ remains invariant in confining phase. Whereas, in the deconfined phase $\langle L(\vec{x})\rangle \neq 0$, thus it is *not* invariant under $Z(3)$ transformations. Thus we conclude that the discrete $Z(3)$ symmetry is spontaneously broken in the deconfined QGP phase. There are 3 equivalent phases in the high temperature phase characterized by values of $\langle L(\vec{x})\rangle$, $Z\langle L(\vec{x})\rangle$ and $Z^2\langle L(\vec{x})\rangle$. Note that the $Z(3)$ symmetry is spontaneously broken in the QGP or the high temperature phase but it's restored in the low temperature or the confined phase. This is in contrast to usual situations in condensed matter systems where the symmetry is restored in the high temperature phase. In view of discussion of section 2.1.1 we note that there will be topological domain wall defect can exist. These corresponds to interpolation of Polyakov loop order parameter field between different $Z(3)$ vacua. We will discuss details of these $Z(3)$ domain wall defects further below.

2.2.3 Effective potential for Order Parameter

In the following, we will suppress the vector indices on $\vec{x}$ and use $l(x)$ for the thermal expectation of Polyakov loop. We will use the effective Lagrangian for the Polyakov

loop as proposed by Pisarski [20, 21],

$$\mathcal{L} = \frac{N}{g^2}|\partial_i l|^2 T^2 - V(l), \tag{2.19}$$

where

$$V(l) = \left(-b_2|l|^2 + b_3(l^3 + (l^*)^3) + |l|^4\right) b_4 T^4. \tag{2.20}$$

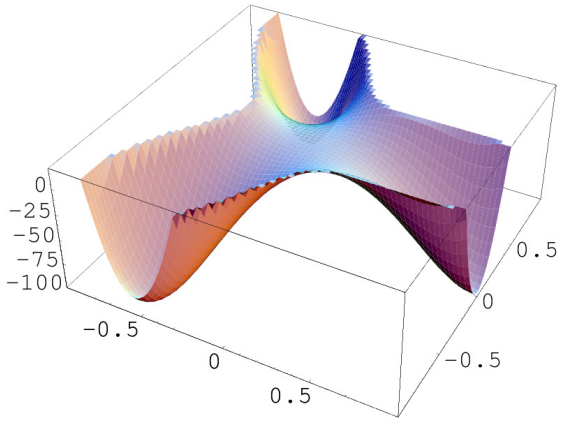

Figure 2.3: Surface plot of potential in the complex $l(x)$ plane for $T = 400$ MeV.

Since l is dimensionless, dimensions of the potential is made up by the factor T^4. In the mean field theory, b_4 is taken as constant and b_2 varies with temperature. For $b_3 \neq 0$, the Lagrangian has $Z(3)$ symmetry. The parameters are fitted in ref. [22–24] such that the effective potential reproduces the thermodynamics of pure $SU(3)$ gauge theory on lattice [25, 26]. The coefficients are taken as $b_2 = (1 - 1.11/x)\,(1 + 0.265/x)^2\,(1 + 0.300/x)^3 - 0.478$, (with $x = T/T_c$ and $T_c \sim 182$ MeV), $b_3 = 2.0$ and $b_4 = 0.6061 \times 47.5/16$. With these values, $l\,(x) \longrightarrow y = b_3/2 + \frac{1}{2} \times \sqrt{b_3^2 + 4b_2\,(T = \infty)}$ as $T \longrightarrow \infty$. Various quantities are then rescaled such that $l\,(x) \longrightarrow 1$ as $T \longrightarrow \infty$. The scaling are

$$l\,(x) \to \frac{l\,(x)}{y}, \quad b_2 \to \frac{b_2}{y^2}, \quad b_3 \to \frac{b_3}{y}, \quad b_4 \to b_4 y^4. \tag{2.21}$$

The surface plot of potential in the complex $l(x)$ plane for $T = 400\ MeV$ is shown in figure 2.3. At low temperature where $l = 0$, the potential has only one minimum.

For temperatures higher than T_c, $l(x)$ develops a non vanishing vacuum expectation value l_0, and the cubic term above leads to three degenerate $Z(3)$ vacua.

2.2.4 $Z(3)$ Domain Wall Defect in C.D. Transition

In the previous section we have discussed the formation of topological defects in the case of spontaneous symmetry breaking phase transition via Kibble mechanism. Application of this for the case of spontaneous breaking of $Z(3)$ symmetry in QCD has been discussed in the literature and the numerical simulation results show that in relativistic heavy-ion collisions typically several large domain wall defects are expected to form in a typical event [27–29]. Basic physical picture of the formation of these $Z(3)$ walls is as follows. In the case of confinement deconfinement phase transition, the $Z(3)$ symmetry is restored in the low temperature phase and it is broken spontaneously in the high temperature phase. Consider effective potential for the Polyakov loop order parameter as given in Eq. 2.20. There are three degenerate minima for temperature higher than T_c. The order parameter field chooses any of these there minima randomly in different regions of space (typically separated by correlation length). Hence domains with different l, $l = 1, e^{i2\pi/3}, e^{i4\pi/3}$ are formed. This leads to formation of $Z(3)$ domain walls in between domains corresponding to different $Z(3)$ vacua. Also, the junction of three domain walls will give rise to topological string, known as the QGP string. Using the techniques used in reference [27] we have calculated the profile of l (domain wall) between different domains for the case of confinement deconfinement phase transition. Figure 2.4 shows the profile of domain wall between two $Z(3)$ domains and the QGP String at the junction of three interfaces.

In Eq. 2.10 we can see that $L(\vec{x})$ is essentially the condensation of background gauge field (A_0). It has been discussed in the literature [30] that this background gauge field leads to CP violating effects for quarks interacting with the wall. This will play an essential role in our calculations of the interaction of quarkonia with these $Z(3)$ walls. We will briefly discuss how to calculate the gauge field A_0 from the Polyakov loop order parameter associated with a given $Z(3)$ wall.

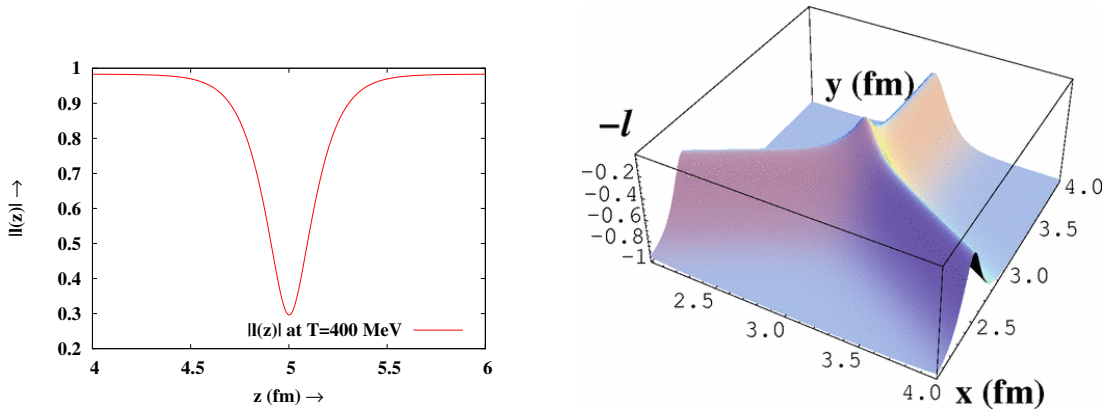

(a) (b)

Figure 2.4: (a):Profile of Domain Wall between two $Z(3)$ domains. (b): QGP String at the junction of three interfaces.

2.2.5 Calculating A_0 Profile for $Z(3)$ Domain Wall

To calculate the A_0 profile we follow the work in ref. [30]. We invert Eq.(2.10) to calculate the A_0 profile form $L(\vec{x})$ profile. We choose A_0 to be of the form

$$A_0 = \frac{2\pi T}{g}\left(a\lambda_3 + b\lambda_8\right), \tag{2.22}$$

where, g is the coupling constant and T is the temperature. λ_3 and λ_8 are the diagonal Gell-Mann matrices. The coefficients a and b depend only on spatial coordinates. The advantage of taking the diagonal gauge choice is that we deal with the eigenvalues of the matrices that are invariant under gauge transformations.

Substituting eq.(2.22) in eq. (2.10), we get

$$3L(x) = \exp(i\alpha) + \exp(i\beta) + \exp(i\gamma), \tag{2.23}$$

where, $\alpha = 2\pi\left(a+b\right)$, $\beta = 2\pi\left(-a+b\right)$ and $\gamma = 2\pi(-2b)$. Here a and b are rescaled like $a \to a/2$ and $b \to b/(2\sqrt(3))$. On comparing the real and imaginary part of Eq. (2.23), we get

$$\cos\left(\alpha\right) + \cos\left(\beta\right) + \cos\left(\gamma\right) = 3|L|\cos\left(\theta\right), \tag{2.24a}$$

$$\sin\left(\alpha\right) + \sin\left(\beta\right) + \sin\left(\gamma\right) = 3|L|\sin\left(\theta\right). \tag{2.24b}$$

In eq. (2.10), A_0 appears as a phase, implies it has $2\pi n$ degeneracy so any increment or decrement in the value of A_0 by a factor of $2\pi n$ will result in the same value of

$L(\vec{x})$. Eq. (2.24), when solved for $|L| = 1$ and $\theta = 0$, give a set of pairs (a, b) as the solutions. Since all these solutions reflect $2\pi n$ ambiguity in A_0, we choose any of the pair and set it as the initial condition. Here we have chosen $(a, b) = (-1.5, -1.0)$.

To calculate A_0 by inverting Eq. (2.24), we choose the continuity of A_0 across the domain wall. This is a crucial ingredient in the numerical scheme that we have used to determine the profile of a, b and hence, A_0. A small region was chosen near the initial a, b and then $|L|$ was calculated for all values in that region. We have taken only those values of a and b were the error between the calculated $|L|$ and $|L|$ obtained by energy minimization was minimum. The process was then repeated for each value of z to obtain a, b values as functions of z. We have compared the calculated $|L|$ profile and the one obtained by energy minimization and shown in figure (2.5a). Figure (2.5b) shows the profile of parameters a and b across the domain wall. The calculated

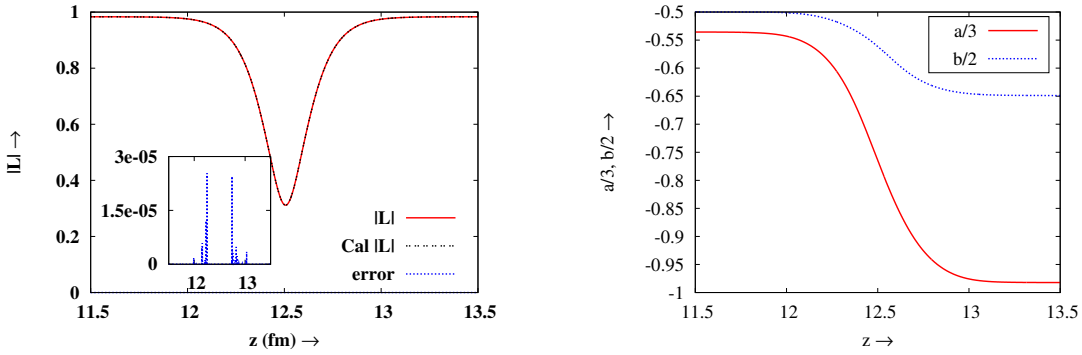

(a) (b)

Figure 2.5: (a): Plot of calculated $|L|$ from a & b and the one obtained from minimizing the energy. The inset figure shows the deviation between the two profiles. (b): Profile of a and b between the regions $L(\vec{x}) = 1$ and $L(\vec{x}) = e^{i2\pi/3}$ with initial point $(-1.5, -1.0)$. Figure taken from [30].

a, b were then used to calculate A_0 using eq (2.22). The A_0 profile was fitted to the function $A_0(x) = p\tanh(qx + r) + s$ using gnuplot. The calculated A_0 profile, fitted A_0 profile and their difference is plotted in figure (2.6).

In the next chapter we will focus on the QGP phase and discuss the formation and evolution of QGP in relativistic heavy-ion collisions and various experimental signatures which have been proposed to detect the transient early stage of QGP.

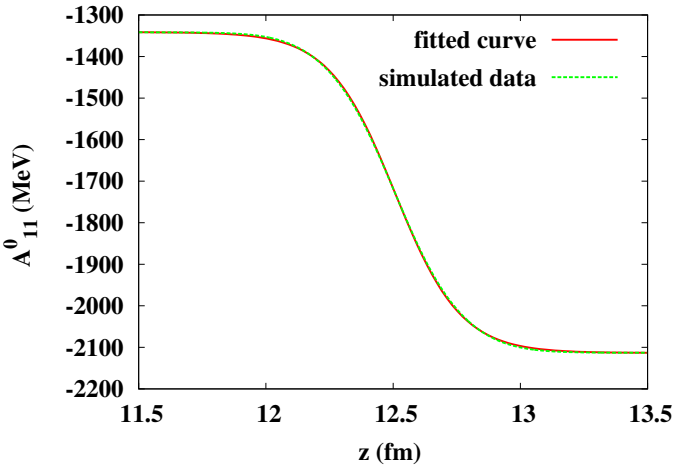

Figure 2.6: Plot of calculated A_0 and the fitted profile ($A_0(x) = p\tanh(qx + r) + s$). The parameters have values $p = -378.27$, $q = 7.95001$, $r = -49.7141$, $s = -1692.48$. Only $(1, 1)$ component of A_0 is plotted. The other components also have similar fit.

Chapter 3

QGP in Laboratory and its Signature

The only way to produce QGP in laboratory is to collide two relativistic heavy nuclei. In these relativistic heavy ion collision experiments (RHICE), heavy nuclei (like gold, lead or copper) are accelerated to ultra relativistic energies with at least few hundreds of GeV per nucleon (in case of LHC their energies are of the order of TeV) and then are collided with each other. At these energies the nuclei get Lorentz contracted in the direction of the boost. The contraction factor is proportional to energy and is equal to $\frac{Average\ Energy\ per\ nucleon}{nucleon\ mass}$, which is few hundred for RHIC and of the order of thousand for LHC. The nuclei of size about $10-12\ fm$ should looks like a $2-D$ disc in the laboratory frame. But instead of a $2-D$ disc it looks like a thin pancake of thickness $\sim 1\ fm$ because of quantum fluctuations.

3.1 Evolution of Medium

After collision, the produced parton system undergoes different stages of evolution, which are characteried as the stages of pre-equilibrium, thermalization, hadronization and subsequently chemical then thermal freezeout. Finally hadrons are detected in the detectors. The evolution of the partonic system in these stages is as follows (see figure 3.1):

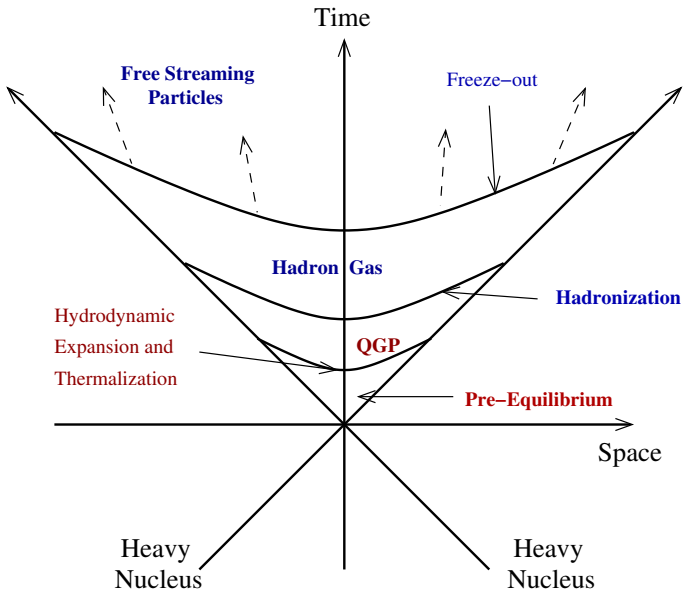

Figure 3.1: A schematic diagram showing various stages of evolution in Heavy Ion Collisions

3.1.1 Pre-Equilibrium and Thermalization

At the time of initial collision of hadrons (hence of partons), due to very high energies, the strong interaction coupling constant becomes very small. As a result the quarks and gluons inside the nucleons interact little due to asymptotic freedom. Hence when the nuclei collide, they essentially pass through each other with negligible interaction as if they are transparent. However, the coupling is not exactly zero, and this leads to copious production of secondary partons in the overlapping region of the nuclei as they pass through each other. Hard collisions also lead to some of the partons getting stopped in the overlapping region, leading to non-zero (though small) baryonic chemical potential of the produced parton system. This sets up the initial conditions or the pre-equilibrium stage for the formation of QGP in laboratory. Still there is no successful model to fully explain this non-equilibrium stage of collision. The modeling of these initial conditions itself is very challenging. There are different types of initial conditions used. One uses the Color Glass Condensate (CGC) model, the Glauber initial conditions and string decays, parton cascade etc. Different models have their own advantages and limitations. Intensive research is going on to understand detailes of these initial conditions. Due to very high density of particle in the overlap region,

they undergo multiple interactions and rapidly attain thermal equilibrium. Various calculations lead to estimate of the thermalization time of about 0.25 fm for RHIC and 0.1 fm for LHC [31]. From experimental side, elliptic flow data [32] requires hydrodynamic evolution with thermalization time to be less than about 1 fm.

3.1.2 Local Equilibration, Plasma Expansion, and Hadronization

As the two receding nuclei move rapidly away from each other, the initial partonic system fills up the region in between them, undergoing rapid longitudinal expansion. There is no transverse expansion initially. After local equilibration the pressure of the system leads to build up of expansion in the transverse direction, though it remains small in comparison to longitudinal expansion. Only at very late stages the expansion becomes more or less isotropic. As the system expands, its temperature drops and finally when the temperature of the system falls below the quark-hadron transition temperature, the system hadronizes. Subsequently, the system of hadron gas evolves with time as the temperature keeps dropping down.

3.1.3 Chemical freeze-out

Initially (just after Hadronization) the produced hadrons have high enough scattering cross section (as the density and/or temperature is high enough) to undergo inelastic collisions. In that stage hadrons interacts and change their chemical composition. With the expansion of the system the temperature and density of the hadron gas decreases and consequently inelastic scattering rate decreases. After certain time the inelastic scattering becomes insignificant and the chemical composition of the system does not change any further (other than the decay of particles). This is known as the stage of chemical freeze-out. We can use the statistical thermal models to described the chemical freeze-out stage with well defined system parameters such as chemical freeze-out temperature T_{ch} and baryon chemical potential μ_B at the feeze-out stage. Still after chemical freeze-out elastic collisions take place and momentum distribution of the system changes.

3.1.4 Thermal Freeze-out

As the system keeps expanding, after some time the expansion rate will exceed the rate of scattering. This means that the momentum distribution of the particles will not change further and they will move freely to the detector. As different species with different mass and interaction rates will have different mean free paths, they will decouple at different times.

3.2 Signature of QGP

After thermal freeze-out hadrons are detected in the detector. We cannot detect the existence QGP phase directly by any detector. Only way is to find certain signatures that QGP existed during an earlier stage of the system evolution. One has to make theoretical models of the phases at earlier stage and predict the signature of the early transient QGP phase in terms of properties of hadrons which can be detected in the detectors. Verification of these predictions with experimental data will give information about these early stages. Though there is no single unique signal which allows a straightforward identification of the quark-gluon plasma phase but accumulative set of signals taken together may provide the indication of the presence of the deconfined phase of matter. Here briefly we will discuss some of the signatures, in particular the signal of suppression of J/ψ. In the next section we will discuss the conventional mechanism of this signature of J/ψ suppression in more detail.

3.2.1 Dilepton Production in the Quark-Gluon Plasma

In the quark-gluon plasma, quark/anit-quark interactions can lead to formation of virtual photons γ^*, which subsequently decay into a lepton-antilepton pair (l^- l^+). The produced lepton-antilepton pair is called a dilepton. The interaction of those particles with medium is electromagnetic interaction, which is suppressed by a factor $(\frac{\alpha_e}{\sqrt{s}})^2$, where α_e is fine structure constant and $\sqrt{s}$ is the charged lepton center-of-mass energy. Accordingly, the mean-free path of the leptons are expected to be larger than the size of the medium produced. So they will likely reach the detector without further interaction with medium. The production and momentum distribution of those

dileptons depends on the momentum distribution of quarks/antiquarks in medium which is governed by the thermodynamics of the medium. Hence dileptons carry the thermodynamic information of the medium at the moment of their production.

3.2.2 Direct Photon Production

In the quark-gluon plasma, a quark and antiquark can interact via each other to produce a photon and a gluon. Also a quark (or an antiquark) can interact with a gluon to produce a photon and a quark (or an antiquark). The first one is known as annihilation processes and the other one is the as Compton processes which is analogous to Compton process in quantum electrodynamics. The analogous electromagnetic process for the first case is $q\ \bar{q} \rightarrow \gamma\ \gamma$ is allowed but suppressed by a factor $\frac{\alpha_e}{\alpha_s} \sim 0.02$. Where α_e is electromagnetic fine structure constant $\frac{e^2}{4\pi}$ and α_s is related to strong coupling constant (g) as $\alpha_s = \frac{g^2}{4\pi}$. In both the processes a photon is produced in medium. As it interacts with the medium only via electromagnetic interaction, same as dilepton, it reaches detector without further interaction. As the production and momentum distribution of produced photon also governed by the thermodynamic condition of the medium through source quarks and gluons, it also carries the thermodynamical properties of the medium at their production time.

Both the above signals have been observed in RHICE [33–35]. However Hadronic interaction can also produce di-lepton pairs or photons. Therefore to separate out the portion of production of di-lepton and photon in QGP, it is necessary to analyze the contributions of other sources.

3.2.3 Strangeness Enhancement

In nucleon-nucleon collisions, all the light quark-antiquark pairs (like $u\bar{u}$, $b\bar{b}$, $s\bar{s}$) are expected to be produced, including the strange quarks. Afterwards the strange quarks and antiquarks combine with other antiquarks and quarks to form strange hadrons. Experimentally the ratio of strange hadron and non-strange hadron are found to be 0.08 [36] for $p - Be$ collision and 0.05 for pp collision. For the case of heavy ion collision this ratio is enhanced. First observation was from NA57 collaboration of SPS at 158 GeV/A energies [37]. Subsequently STAR collaboration at RHIC also

observed the same phenomena [38, 39]. This indicates that there is another source of $s\bar{s}$ production than purely hadronic interactions [40, 41]. If there is a QGP medium then thermal $s\bar{s}$ can be produced. Hence the enhancement of strange hadrons for heavy-ion collisions compared to $p - Be$ and pp collisions indicates existence of an intermediate deconfined phase of matter.

3.2.4 Elliptic Flow

This is the strongest signal of QGP as a thermalized system. It arises from the fact that non-central collisions will give rise to spatially anisotropic medium arising from the geometry of the overlapping region of the colliding nuclei. Consequently, the pressure gradients will be different in different azimuthal directions. Hydrodynamic evolution of this syetm will lead to momentum anisotropy of final state particles. Consequently, the second Fourier coefficient (called as elliptic flow) of the azimuthal distribution of particles will be non-zero. This has been observed experimentally in RHIC and LHC experiments [42]. Hydrodynamical simulations [43–45] show that the observed anisotropy can be explained only when there is a QGP medium, with thermalization time smaller than 1 fm and with a small value of η/s. The elliptic flow of partons reflects the momentum anisotropy of thermalized quarks [46–49].

3.2.5 Jet Quenching

In deep inelastic scattering processes, due to hard scattering, pairs of jets, with partons moving in opposite directions are produced. The jet that propagate through the dense and hot matter suffers re-scattering thus loses energy and finally gets absorbed in that medium. The other jet moving in opposite direction which suffers less interaction that propagate outside the medium can be detected. This effect is known as jet quenching which indicates the presence of a hot and dense medium. This was first observed at RHIC [50, 51] then subsequently at LHC also [52]. This quenching of jet carries information about the hot and dense medium.

3.2.6 Quarkonia Suppression

Quarkonia, the bound state of heavy quark (q) and antiquark ($\bar{q}$), are produced at the early stages of the heavy-ion collision. There are two types of quarkonia which can be produced at presently available accelerators enrgies, charmonia (bound state of charm and anticharm) like J/ψ, ψ' etc., and bottomonia (bound state of bottom and antibottom) like Υ, $\Upsilon(2S)$ etc. In high energy heavy ion collisions QGP, the deconfined phase of matter, is expected to be produced. With color charges being deconfined, there will be Debye screening of the color charges in the QGP [53]. This screening will weaken the binding of quark-antiquark system. If the screening is sufficient, quarkonia will not be bound any more and will melt in the medium. The heavy quark and the antiquark will subsequently combine with other antiquarks/quarks to form open charms (D) and open bottoms (B) during the subsequent hadronization process. This will increase suppression of yield of quarkonia. Matsui and Satz [54] first proposed suppression of yield of J/ψ (and other charmonia) as a signal for the presence of QGP. This has been observed experimentally at SPS in central Pb-Pb collisions [55, 56], and in subsequent experiemnts (though at higher energies, regeneration of quarkonia also becomes important).

As this thesis relates to this particular signal, we will start discussing this in more detail with the potential model picture of quarkonia. We start by considering quarkonia as a two body system with color charges g and $-g$. The potential energy of the $q\bar{q}$ system, separated by a distance r, coming from one gluon exchange can be represented phenomenologically by the Coulomb potential energy (in analogy with quantum electrodynamics)

$$V_0(r) = -\frac{\alpha}{r} \tag{3.1}$$

The confining part, coming from multi gluon exchange is represent by a term linear in r (in accordance with the string model of confinement)

$$V_c(r) = \sigma r. \tag{3.2}$$

α is related to the strong coupling constant g and σ is the string tension. The potential energy and Hamiltonian for the $q\bar{q}$ system are [57–59]

$$V(r) = -\frac{\alpha}{r} + \sigma r;\ H = \frac{p^2}{2\mu} + V(r) \tag{3.3}$$

where $\mu(=\frac{m_q}{2})$, the reduced mass of the quark antiquark system. The parameters of the Hamiltonian (or the potential) are fixed from the observed spectra of quarkonia. We choose the parameters $\alpha = 0.52,\ \sigma = 0.926\ GeV/fm$ and $m_c = 1.84\ GeV$ and $m_b = 5.17\ GeV$ [57].

In the second step we put the $q\bar{q}$ system in QGP. The QGP consists of thermal quarks and gluons, which will rearrange around the q and $\bar{q}$ and modify the potential between q and $\bar{q}$. This modification of Coulomb part is because of the (Debye) screening of color charges of q and $\bar{q}$. Consequently, the interaction will become short range Yukawa-type interaction. The string tension part also gets modified because of the thermal medium, and eventually vanishes after certain temperature [53,59]. Now, confinement occurs because of the string (linear part in the potential). Therefore, vanishing of the string tension implies deconfinement of quarks and gluons. However, for charmonia or bottomonia, absence of string tension does not automatically give rise the phenomena of melting. They remain bound up to certain temperature (T_d) because of modified (Debye screened) Coulomb interaction (or Yukawa interaction) in medium.

Qualitatively the Debye screening can be understood by approximating the non-abelian color interaction by abelian Coulomb interaction. The phenomena of screening comes from redistribution of thermal charges like quarks and gluons. Consider initially a quark-gluon plasma, in thermal equilibrium at a temperature T, with zero chemical potential. The number density of quarks n_q and antiquarks $n_{\bar{q}}$ are same. The number density of different flavors with mass m_q, at a temperature T, is proportional to the Boltzmann factor $e^{-m_q/T}$. This implies that QGP will consist of mostly u, d and s quarks and antiquarks up to few hundred MeV temperature. In that temperature range the fraction of charm and bottom quark will be very small. Invoking the fact that the string tension part is negligible and the quarks and anti quarks interact via color Coulomb interaction $(-\frac{\alpha}{r})$, any test quark will be surrounded by quarks of opposite charge. This will reduce the visibility of the test quark from others, leading to reduced interaction strength and range. So a heavy quark and antiquark will feel less interaction between them because of the screening. For the case of plasma as a massless quark and antiquark ideal gas, the potential $V(r)$ seen by a test quark at a distance r will be modified from the long-range Coulomb potential to the short-range

Yukawa potential

$$V(r) = -\frac{\alpha}{r} e^{-\frac{r}{\lambda_d}}, \tag{3.4}$$

where λ_d is screening length or Debye length. For the abelian case this is given by [9]

$$\lambda_d = \sqrt{\frac{9 \times 1.202\ T}{\pi^2 q^2 (n_q + n_{\bar{q}})}} \tag{3.5}$$

As in the abelian approximation gauge bosons do not carry color charge, so the screening above does not have any contribution from gauge bosons (gluons). But the contribution from gluons will be non-zero for QCD. Like quarks and antiquarks, gluons also polarize the medium surrounding the test quark. This gives additional screening to the test quark. The Debye mass (inverse of Debye length) from one loop Perturbative QCD (PQCD) calculation (Appendix C of [60]) is given by,

$$m_d(PQCD) = \frac{1}{\lambda_d(PQCD)} = gT\sqrt{1 + \frac{N_c}{6} + \frac{N_f}{3}} \tag{3.6}$$

Here subscript "c" is for color and "f" is for flavor. Now our goal is to find the temperature (T_d) at which the Debye screening will be sufficient to break the quark-antiquark pair. We can estimate that temperature by taking non-relativistic approximation. The Hamiltonian for $q\bar{q}$ system in QGP is

$$H = \frac{p^2}{2\mu} - \frac{\alpha e^{-r/\lambda_d}}{r} \tag{3.7}$$

By semi-classical argument and using the uncertainty relation $\langle p^2 \rangle \sim \frac{1}{r^2}$ we have the energy of the system

$$E(r) = \frac{1}{2\mu r^2} - \frac{\alpha e^{-r/\lambda_d}}{r} \tag{3.8}$$

By minimizing energy ($E(r)$) with respect to r we have the condition for the possible bound state.

$$-\frac{1}{\mu r^3} + \frac{\alpha}{r^2}(1 + r/\lambda_d) e^{-r/\lambda_d} = 0 \tag{3.9}$$

or

$$x(x+1)e^{-x} = (\alpha\mu\lambda_d)^{-1} \tag{3.10}$$

where $x = r/\lambda_d$. The above equation has a solution only if $(\alpha\mu\lambda_d)^{-1} \leq 0.84$. Implies

$$\lambda_d^{min} = \frac{1}{0.84\ \alpha\mu} \tag{3.11}$$

is the smallest value of Debye length which permits bound state. Eq.(3.9) in the limit $\lambda_d \to \infty$ provides us the Bohr radius at zero temperature, which is $r_{Bohr} = 1/(\alpha\mu)$ From Eq.(3.11) we can say, $q\bar{q}$ will not be bound if $1.19 r_{Bohr} > \lambda_d$. For J/ψ taking $\alpha = 0.52$ and $m_q = 1.84$ we get Debye length at $T = 200\ MeV$ to be $\lambda_d(PQCD) = 0.36\ fm$ and $r_{Bohr} = 0.41\ fm$. This indicates that at $T = 200\ MeV$ this $q\bar{q}$ system will not be bound. Using Eq.3.6 and 3.11 we have the dissociation temperature

$$T_d = 0.84\ \mu\sqrt{\frac{2\alpha}{9\pi}} \tag{3.12}$$

which is about 150 MeV for $\alpha = 0.52$.

Though the values are not very reliable, with the crude picture used here, qualitatively we conclude that there will be a maximum temperature (T_d) for QGP, above which there won't be any bound quarkonia. So the suppression in the yield of quarkonia will indicate the creation of QGP in heavy ion collision. Experimental results [56] show a suppression of J/ψ with number of participants (N_{part}). This is consistent with the expectation of J/ψ suppression in the QGP medium.

However, there are other factors too that can lead to the suppression of J/ψ because of which it has not been possible to use J/ψ suppression as a clean signal for QGP like, J/ψ suppression in Hadronic medium. One also observes stronger suppression for forward rapidity than on the mid rapidity at RHIC [61, 62] as well as at LHC [63]. Using the same picture Υ suppression is proposed as a signal and it has been observed in ALICE collaboration [64]. This does not have such issues like anomalous suppression in different rapidity region.

Chapter 4

Evolution of States Under Time-Dependent Perturbation Theory

This thesis primarily concerns the evolution of quarkonia states under changes in potential between quark and antiquark in the QGP medium produced in RHICE. The change in the potential can originate from the interaction of the quarkonia with $Z(3)$ domain walls, or it can occur during thermalization of the medium produced in RHICE and also during the evolution of the thermalized medium of QGP. Here we will discuss the evolution of quarkonia states using time-dependent perturbation theory. We will discuss the validity of adiabaticity during the evolution of quarkonia states and discuss the opposite limit of sudden approximation for the perturbation. We will also check the error in the use of sudden approximation. We start with brief review of the evolution of quantum states under time dependent perturbation.

4.1 Time-Dependent Perturbation Theory

In the case of time-independent perturbation theory we calculate how the eigen states and corresponding eigen values of unperturbed Hamiltonian gets modified due to the presence of a perturbation. When perturbation depends on time then the Hamiltonian changes with time, consequently there would not be any stationary states. So in this

case we are not suppose to talk about only the modification of eigen states. Rather, we are interested in the evolution of initial states under the action of this time dependent perturbation.

Consider the time-dependent Hamiltonian as

$$H = H_0 + V(t) \tag{4.1}$$

Where H_0 is the constant (in time) part of the Hamiltonian whose eigen values (E_n) and eigen functions ($|n(t)\rangle = e^{-iE_nt}|n\rangle$) are exactly known, and $V(t)$ is small perturbation in comparison to the original Hamiltonian

Now if at initial time ($t = 0$), the system is in the eigen state $|i(0)\rangle$ of H_0 and we let the system evolve under this perturbation then we want to find what is the probability that the system can be found in state $|f(t)\rangle$ at some later time t. Let us assume that at time t the initial state evolved to a state $|\psi(t)\rangle$. We can always expand $|\psi(t)\rangle$ in terms of the eigen state $|n(t)\rangle$ of H_0, as it forms a complete set of orthonormal basis.

$$|\psi(t)\rangle = \sum_n c_n(t)|n(t)\rangle. \tag{4.2}$$

The probability that the state $|\psi(t)\rangle$ make a transition to the state $|f(t)\rangle$ can be found by taking projection of $|\psi(t)\rangle$ on $|f(t)\rangle$. Taking $|f(t)\rangle$ to be an eigen state of H_0, this gives

$$\langle f(t)|\psi(t)\rangle = c_f(t). \tag{4.3}$$

Since $|n(t)\rangle$ are eigen states of H_0, they satisfy time dependent Schrödinger equation

$$i\frac{\partial}{\partial t}|n(t)\rangle = H_0|n(t)\rangle, \tag{4.4}$$

Schrödinger equation corresponding to the perturbed Hamiltonian H is

$$i\frac{\partial}{\partial t}|\psi(t)\rangle = H|\psi(t)\rangle \tag{4.5}$$

Using Eq.(4.1), Eq.(4.2) and Eq.(4.4), we obtain

$$i\sum_n(\frac{\partial}{\partial t}c_n(t))|n(t)\rangle = \sum_n V(t)c_n(t)|n(t)\rangle \tag{4.6}$$

Multiplying both side of the above equation by $\langle f(t)|$ and integrating one can get the relation

$$i\frac{\partial}{\partial t}c_f(t) = \sum_n V_{fn}(t)c_n(t), \tag{4.7}$$

where

$$\begin{aligned} V_{fn}(t) &= \langle f(t)|V(t)|n(t)\rangle \\ &= V_{fn}e^{i\omega_{fn}t} \end{aligned} \tag{4.8}$$

and

$$V_{fn} = \langle f|V(t)|n\rangle \ , \ \ \omega_{fn} = E_f - E_n \tag{4.9}$$

Since we have taken the initial state $|i(t)\rangle$ also to be an eigen state of H_0, this implies that at zeroth order (in perturbation V) the amplitude $c_n^{(0)} = \delta_{in}$. Then, up to first order ($O(V)$) Eq.(4.7) becomes

$$\dot{c}_f^{(1)}(t) = -iV_{fi}e^{i\omega_{fi}t}. \tag{4.10}$$

Integrating this equation, we have

$$c_f^{(1)}(t) = -i\int_0^t V_{fi}e^{i\omega_{fi}t'}dt' \tag{4.11}$$

The expression for complete first order amplitude is

$$\begin{aligned} c_f(t) &= c_f^{(0)}(t) + c_f^{(1)}(t) \\ &= \delta_{fi} - i\int_0^t V_{fi}e^{i\omega_{fi}t'}dt' \end{aligned} \tag{4.12}$$

Hence the probability of transition up to first order from initial state $|i(t)\rangle$ to a final state $|f(t)\rangle$ is

$$\begin{aligned} P_{fi}(t) &= |c_f(t)|^2 \\ &= |\delta_{fi} - i\int_0^t V_{fi}e^{i\omega_{fi}t'}dt'|^2 \end{aligned} \tag{4.13}$$

4.1.1 Transition Under Perturbation Acting for Finite Time

In many cases the time dependent Hamiltonian never goes to its original value. Perturbation starts at $t = 0$ and remains non-zero even after a finite time t. In that case at $t \to \infty$ right hand side (RHS) of Eq.(4.11) diverges. So this formula for transition from one state to other state can not be applied directly. Physically this divergence

is not important for our case and this can be removed easily (see, ref. [65] for details). To do this, we integrate RHS of Eq.(4.11) by parts:

$$\begin{aligned} c_f^{(1)}(t) &= -i\int_0^t V_{fi}e^{i\omega_{fi}t'}dt' \\ &= -\left[\frac{V_{fi}e^{i\omega_{fi}t'}}{\omega_{fi}}\right]_0^t + \int_0^t \frac{\frac{\partial V_{fi}}{\partial t}e^{i\omega_{fi}t'}}{\omega_{fi}}dt' \end{aligned} \tag{4.14}$$

Since at $t = 0, V(t) = 0$ implies at $t = 0$ first term vanishes, while at t this term this term gives the contribution of the modification in the states under the action of time independent perturbation up to first order correction (with the exponential factor $e^{i\omega_{fi}t}$ giving the corresponding time dependence). That means if we expand $V(t)$ in Taylor seres about $V(0)$ up to first order then at $t \to \infty$ the first term corresponds to the constant part of the perturbation $V(\infty)$, while the second term corresponds to the time varying part giving transition to other states. Thus, the probability of transition to other states will be given by ([65])

$$P_{fi}(t) = \frac{1}{\omega_{fi}^2}|\int_0^t \dot{V}_{fi}e^{i\omega_{fi}t}dt|^2. \tag{4.15}$$

If $\dot{V}(t)$ is sufficiently small during the relevant time interval (meaning that the perturbation $V(t)$ varies slowly) then the second term will be negligible compared to the first term in Eq.4.14. Thus if we apply perturbation sufficiently slowly (*adiabatically*), a system will remain in that state. For that the system has to be in a non-degenerate stationary state. In Sec.(4.2) the above scenario will be discussed in more detail.

4.2 Adiabatic Evolution of States

In heavy-ion collisions one often uses adiabatic evolution of states in any change of Hamiltonian (during thermalization of the medium after collision, during freezeout etc.). Origin of the word "Adiabatic" is a Greek word adiabatos 'impassable', from a- 'not' + dia 'through' + batos 'passable' (from bainein 'go'), was introduced by Nicolas Lèonard Sadi Carnot in 1824 to explain Carnot heat engine. In the present context, adiabatic evolution means gradually changing conditions allowing the system to adapt its configuration. In such evolution process, a state with an initial Hamiltonian will

evolve with time to the corresponding eigen state of final Hamiltonian. That means if a Hamiltonian changes continuously from $H(t_0)$ to $H(t)$ and we let the the initial state, $|n(t_0)\rangle$ which is an eigen state of $H(t_0)$, to evolve adiabatically then it will reach a final state $|n(t)\rangle$, the corresponding eigen state of $H(t)$. In previous section qualitatively we have discussed the condition for adiabatic evolution. Now quantitatively we will find the condition for adiabatic evolution. For a time-dependent Hamiltonian H, the instantaneous eigen functions ($|n(t)\rangle$) and eigen values ($E_n(t)$) are given as

$$H(t)|n(t)\rangle = E_n(t)|n(t)\rangle \tag{4.16}$$

At any instant of time these states form a complete orthonormal basis. So one can expand any general solution $|\psi(t)\rangle$for schrödinger equation

$$i\frac{\partial}{\partial t}|\psi(t)\rangle = H(t)|\psi(t)\rangle \tag{4.17}$$

in terms of that basis as

$$|\psi(t)\rangle = \sum_n c_n(t)|n(t)\rangle e^{i\theta_n(t)} \tag{4.18}$$

where

$$\theta_n(t) = -\int_0^t E_n(t')dt' \tag{4.19}$$

Substituting Eq.(4.18) into the Eq.(4.17) and using the relation Eq.(4.16) we have

$$i\sum_n \left(\dot{c}_n|n\rangle + c_n|\dot{n}\rangle + ic_n|n\rangle\dot{\theta}_n\right)e^{i\theta_n} = \sum_n c_n E_n|n\rangle e^{i\theta_n} \tag{4.20}$$

After taking derivative on both side of Eq.(4.19) we can show that last term of LHS is equal to RHS. This implies

$$\sum_n \dot{c}_n|n\rangle e^{i\theta_n} = -\sum_n c_n|\dot{n}\rangle e^{i\theta_n} \tag{4.21}$$

Multiplying $\langle m|$ from left and after simplification we obtain

$$\dot{c}_m = -\sum_n c_n\langle m|\dot{n}\rangle e^{i(\theta_n-\theta_m)} \tag{4.22}$$

Taking derivative on both side of Eq.(4.16) we get

$$\dot{H}|n\rangle + H|\dot{n}\rangle = \dot{E}_n|n\rangle + E_n|\dot{n}\rangle. \tag{4.23}$$

Multiplying $\langle m|$ from left and using the relation $\langle m|H = E_m\langle m|$ we have for $m \neq n$

$$\langle m|\dot{H}|n\rangle = (E_n - E_m)\langle m|\dot{n}\rangle. \tag{4.24}$$

Finally we have

$$\dot{c}_m = -c_m\langle m|\dot{m}\rangle - \sum_{n\neq m} c_n \frac{\langle m|\dot{H}|n\rangle}{(E_n - E_m)} e^{i(\theta_n - \theta_m)}. \tag{4.25}$$

For adiabatic limit (when H varies slowly) we can drop the second term at the RHS of the above equation, then we obtain

$$\dot{c}_m = -c_m\langle m|\dot{m}\rangle. \tag{4.26}$$

When the system starts from the state $|i\rangle$ initially, the boundary condition $c_n(0) = \delta_{in}$ implies the solution of the Eq. 4.26

$$c_i = c_i(0)e^{\gamma_i(t)} \tag{4.27}$$

where

$$\gamma_i(t) = i\int_0^t \langle i(t')|\frac{\partial}{\partial t'}|i(t')\rangle dt' \tag{4.28}$$

So the final state can be written as

$$|\psi(t)\rangle = e^{\gamma_i(t)}e^{\theta_i(t)}|i(t)\rangle \tag{4.29}$$

$\theta_i(t)$ and $\gamma_i(t)$ are known as dynamical and geometric phase, respectively. Hence the final state is nothing but the ith eigen state of the Hamiltonian $H(t)$ at time t with a phase factor. We say that the adiabatic approximation is valid when the following condition (expressed in terms of dimensionless ratio) is satisfied [66],

$$\frac{|\langle m|\dot{H}(t)|n\rangle|}{(E_n - E_m)^2} \ll 1 \tag{4.30}$$

Or

$$\left(\frac{\tau_e}{\tau_m}\right)^2 \ll 1 \tag{4.31}$$

Where τ_e gives an estimate of the transition time scale between different states (being inverse of the characteristic energy gap between different energy eigenstates of the system), whereas τ_m corresponds to the time scale of the evolution of the Hamiltonian. The above ratio is a measure of adiabaticity, which should be much less than 1 in order to allow the adiabatic evolution of states of the quantum mechanical system.

4.3 Sudden Perturbation

Consider another limiting case when perturbation changes abruptly over a very small time interval τ. From Eq.(4.5) one can write

$$\delta|\psi(t)\rangle = H|\psi(t)\rangle\delta t \tag{4.32}$$

As the time interval is infinitesimally small and $H|\psi(t)\rangle$ is finite in that duration of time, one can say $\delta|\psi(t)\rangle \sim 0$. Wave function remains unchanged on action of sudden perturbation. We solve the instantaneous eigen states of H, before and after that instant. Using the fact that the initial state $|n(0)\rangle$ remains unchanged, the final state, which is nothing but the initial state, is no longer eigen states of final Hamiltonian of the system, i.e. the state will not be a stationary states and will, in general, be a linear combination of the stationary states $|n'(t)\rangle$ of final Hamiltonian H. So the overlap of $|n(0)\rangle$ with the new stationary eigen states $|n'(t)\rangle$, gives us the probability of its transition to other states. The probability of transition from initial state $|i\rangle$ of H_0 to a final state $|f'\rangle$ of H is

$$P_{fi} = \langle f'|i\rangle. \tag{4.33}$$

The calculation of sudden perturbation is exact, the only approximation is taken here is the time interval of the change of Hamiltonian is infinitesimally small, i.e. the Hamiltonian changes suddenly.

4.3.1 Condition for Sudden approximation and Error Calculation

To find the condition for validity of sudden approximation, we should find the probability ζ that the state does not remain in the original state after action of the perturbation ($V(t)$), which is measure of the error involved in this approximation. Consider the initial state $|i\rangle$ to be an eigen state of H_0. The projection operator orthogonal to that state is $Q = 1 - |i\rangle\langle i|$. $|\psi\rangle$ is the evolved states after action of the perturbation. So ζ can be written as

$$\zeta = \langle\psi|Q|\psi\rangle \tag{4.34}$$

$|\psi\rangle$ can be expanded in terms of the eigen state $|n\rangle$ of H_0.

$$|\psi\rangle = \sum_n c_n |n\rangle \tag{4.35}$$

Where the expansion coefficients c_n's can be found using perturbation theory. Using first order perturbation theory Eq.(4.12 & 4.8). We have,

$$c_n = \delta_{ni} - i \int_0^\tau \langle n|V(t)|i\rangle dt \tag{4.36}$$

In the above integration one can take outside the integral the comparatively slowly varying function $|i\rangle$ & $|n\rangle$ and use the instantaneous values. The integral is then found to be

$$\begin{aligned} c_n &= \delta_{ni} - i\tau\langle n| \left(\frac{1}{\tau}\int_0^\tau V(t)dt\right)|i\rangle \\ &= \delta_{ni} - i\tau\langle n|\bar{V}|i\rangle \end{aligned} \tag{4.37}$$

Where

$$\bar{V} = \frac{1}{\tau}\int_0^\tau V(t)dt \tag{4.38}$$

Using equations (4.34, 4.35, 4.37 & 4.38) and after simplification we have

$$\zeta = \tau^2\langle i|\bar{V}Q\bar{V}|i\rangle + O(\tau^3) \tag{4.39}$$

As we have consider the value of c_n corrected up to first order which is order of τ and ζ is second order in c_n, ζ is correct up to order τ^2. Since

$$\langle i|\bar{V}Q\bar{V}|i\rangle = \langle i|\bar{V}^2|i\rangle - \langle i|\bar{V}|i\rangle^2 = \left(\Delta\bar{V}\right)^2 \tag{4.40}$$

where $\Delta\bar{V}$ is the root mean square deviation of the observable $\bar{V}$ in the state $|i\rangle$, so we have the error in sudden approximation calculation

$$\zeta = \tau^2(\Delta\bar{V})^2 + O(\tau^3) \tag{4.41}$$

Hence the condition for the validity of the sudden approximation, $\zeta \ll 1$ implies

$$\tau \ll \frac{1}{\Delta\bar{V}} \tag{4.42}$$

This is nothing but one form of time energy uncertainty relation. We will use the results of this section later in Chapter 7 where we will consider the issue of adiabaticity in the evolution of quarkonia states during the early thermalization of QGP in RHICE.

Chapter 5

A Novel Mechanism of J/ψ Disintegration in Heavy Ion Collisions

We discussed in section 2.2.4 that confinement-deconfinement transition will lead to formation of $Z(3)$ domain walls. We have calculated background gauge field associated with such $Z(3)$ walls in section 2.2.5. Several aspects of these topological domain wall defects have been discussed in literature [30,67,68]. It was shown in ref. [68] that background gauge field A_0 associated with *generalized* $Z(N)$ interfaces can lead to spontaneous CP violation in the Standard Model which, in turn, can lead to baryogenesis in the early universe. A detailed quantitative analysis of this spontaneous CP violation was done in [30], in the context of quark/antiquark scattering from $Z(3)$ walls in the QGP phase. The main approach followed in refs. [30,68] was based on the assumption that the profile of the Polyakov loop order parameter $l(x)$ corresponds to a condensate of the background gauge field A_0 (in accordance with the definition of the Polyakov loop). This profile of the background gauge field is then calculated from the profile of $l(x)$. Such a gauge field configuration in the Dirac equation leads to different potentials for quarks and antiquarks, leading to spontaneous CP violation in the interaction of quarks and antiquarks from the Z(3) wall. This is the origin of spontaneous CP violation from $Z(N)$ walls which was first discussed by Altes et al. [68, 69] in the context of the universe and in ref. [70] for the case of QCD. In [30]

quantitative results were obtained for the profile of A_0 from the profile of Polyakov loop $l(x)$ between different Z(3) vacua (using specific effective potential for $l(x)$ as discussed in [20, 22–24]). This background A_0 configuration acts as a potential for quarks and antiquarks. It was shown in ref. [30] that the quarks have significantly different reflection coefficients than anti-quarks and the effect is stronger for heavier quarks. For a discussion of calculation of A_0 profile, see ref. [30].

In this chapter, we discuss the effect of this spontaneous CP violation on the propagation of quarkonia in the QGP medium, in particular, the J/ψ meson. J/ψ are produced in the initial stages of relativistic heavy ion collisions. As these are heavy mesons ($m \sim 3GeV$), they are never in equilibrium with the QGP medium produced in present heavy-ion collision experiments. However, there are finite T effects (like Debye screening etc.) affecting its motion in a thermal bath. Such effects give rise to the important signal of J/ψ suppression as we discussed in the Introduction. We ignore these effects initially and comment on it towards the end of this chapter. Note that if the Debye length is larger, then the conventional mechanism of J/ψ melting does not work. As we will argue, for large Debye screening length, our mechanism of J/ψ disintegration, discussed in this chapter, works better as any possible screening of the domain wall over the relevant length scale of J/ψ will be small.

If a domain wall is present in the QGP, then a J/ψ moving through the wall will have a non-trivial interaction with it. Due to the CP violating effect of the interface on quark scattering, c and $\bar{c}$ in J/ψ experience different color forces depending on the color of the quark and the color composition of the wall. This not only changes the color composition of $c\bar{c}$ bound state (from color singlet to color octet state) but also facilitates its transition to higher excited states (for example χ states). Color octet quarkonium states are unbound (also, the χ state has larger size than J/ψ and the Debye length), hence they will dissociate in the QGP medium. This summarizes the basic physics of our model discussed in this chapter for quarkonia disintegration due to $Z(3)$ walls [71].

5.1 Interaction of J/ψ with a Z(3) wall

In our model, J/ψ interacts with the gauge field A_0 corresponding to the $l(x)$ profile of the Z(3) wall. This allows for the possibility of color excitations of J/ψ as well as the spatial excitations of its wave function. First we discuss the possibility of color excitations of J/ψ. Subsequently, we will discuss spatial excitations of J/ψ.

5.1.1 Color excitation of J/ψ

We work in the rest frame of J/ψ and consider the domain wall coming and hitting the J/ψ with a velocity v along z-axis. The gauge potential and coordinates are appropriately Lorentz transformed as

$$A_0(z) \to A_0'(z') = \gamma\left(A_0(z) - vA_3(z)\right) \tag{5.1a}$$

$$A_3(z) \to A_3'(z') = \gamma\left(A_3(z) - vA_0(z)\right) \tag{5.1b}$$

$$z = \gamma\left(z' + vt'\right). \tag{5.1c}$$

We assume that there is no background vector potential, $A_i(z) = 0\ ; i = 1, 2, 3$. A_3' obtained from Eq. (5.1b) has only z' dependence, so it does not produce any color magnetic field. Further, using the non-relativistic approximation of the Dirac equation one can see that the perturbation terms in the Hamiltonian (say, $H^1(A_3')$) involving A_3' are suppressed compared to the perturbation term ($H^1(A_0')$) involving A_0' at least by a factor

$$\frac{H^1(A_3')}{H^1(A_0')} \sim \frac{v}{c}\frac{1}{m_c r_{J/\psi}} \tag{5.2}$$

where $r_{J/\psi}$ is the size of the J/ψ wave function and m_c is the charm quark mass. As we will see, the largest value of v/c we consider is 0.20 - 0.24 (above which transition amplitude becomes too large to trust first order perturbation approximation). With $r_{J/\psi} \simeq 0.4$ fm, the suppression factor in Eq. 5.2 is of order 10 %. Thus we neglect perturbation due to A_3' and only consider perturbation due to A_0' as given by Eq.(5.1a). We use first order time dependent perturbation theory to study the excitation of J/ψ due to the background A_0 profile and consider the transition of J/ψ

from initial energy eigenstate ψ_i with energy E_i to the final state ψ_j with energy E_j. The transition amplitude is given by

$$\mathcal{A}_{ij} = \delta_{ij} - \ i \int_{t_i}^{t_f} \langle \psi_j | \mathcal{H}_{int} | \psi_i \rangle e^{i(E_j - E_i)t} dt. \tag{5.3}$$

We take incoming quarkonia to be a color singlet state. The interaction of the quarkonia with the wall is written as

$$\mathcal{H}_{int} = V^q(z_1') \otimes \mathbb{I}^{\bar{q}} + \mathbb{I}^q \otimes V^{\bar{q}}(z_2') \tag{5.4a}$$

$$\text{with} \ \ V^{q,\bar{q}}(z_{1,2}') = g A_0'^{q,\bar{q}}(z_{1,2}'), \tag{5.4b}$$

where $A_0'^{q,\bar{q}}(z_{1,2}')$ is the background field configuration in the rest frame of J/ψ. z_1' and z_2' are the coordinates of q and $\bar{q}$ in quarkonia and g is the gauge coupling. The gauge potential A_0 is taken in the diagonal gauge as

$$A_0 = \frac{2\pi T}{g} \left(a\lambda_3 + b\lambda_8 \right), \tag{5.5}$$

where λ_3 and λ_8 are the Gell-Mann matrices. Under CP, $A_0 \to -A_0$, hence $A_0^{\bar{q}} = -A_0^q$. Now, both the initial and the final states have a spatial, spin and color part. The incoming quarkonia is a color singlet while outgoing state could be a singlet or an octet. Using Eq. (5.4), (5.5) and extracting only the color part of interaction, we get

$$\begin{aligned} \langle \psi_{out} | \mathcal{H}_{int} | \psi_{singlet} \rangle = & \langle \psi_{out} | g A_0'^{q}(z_1') \otimes \mathbb{I}^{\bar{q}} | \psi_{singlet} \rangle \\ & + \langle \psi_{out} | \mathbb{I}^q \otimes g A_0'^{\bar{q}}(z_2') | \psi_{singlet} \rangle. \end{aligned} \tag{5.6}$$

The color singlet state of J/ψ is written as,

$$\begin{aligned} |\psi_{singlet}\rangle = \frac{1}{\sqrt{3}} \Bigg[& \begin{pmatrix} 1 \\ 0 \\ 0 \end{pmatrix}^q \otimes \begin{pmatrix} 1 \\ 0 \\ 0 \end{pmatrix}^{\bar{q}} + \begin{pmatrix} 0 \\ 1 \\ 0 \end{pmatrix}^q \otimes \begin{pmatrix} 0 \\ 1 \\ 0 \end{pmatrix}^{\bar{q}} \\ & + \begin{pmatrix} 0 \\ 0 \\ 1 \end{pmatrix}^q \otimes \begin{pmatrix} 0 \\ 0 \\ 1 \end{pmatrix}^{\bar{q}} \Bigg]. \end{aligned} \tag{5.7}$$

If the outgoing state is also a singlet then, each term on RHS of Eq. (5.6) is zero due to the traceless nature of A_0. Eq. (5.3) gives $\mathcal{A}_{ij} = 1$ for ground state

$(i = j)$. (Meaning, one will then need to resort to 2nd order perturbation theory for consistency). For higher orbital states $(i \neq j)$, amplitude is identically zero. A color octet state like $|r\bar{g}\rangle$, can be written as

$$|r\bar{g}\rangle = \begin{pmatrix} 1 \\ 0 \\ 0 \end{pmatrix}^{q} \otimes \begin{pmatrix} 0 \\ 0 \\ 1 \end{pmatrix}^{\bar{q}} . \tag{5.8}$$

For such an outgoing state each term on RHS of Eq. (5.6) again vanishes identically because of the diagonal form of A_0, resulting in zero transition probability. Same argument leads to zero transition probability to all other octet states with similar color content, viz. $b\bar{g},\ b\bar{r},\ g\bar{r},\ g\bar{b},\ r\bar{b}$. There are only two states with non-zero color contribution to transition probability. They are

$$|r\bar{r} - b\bar{b}\rangle = \frac{1}{\sqrt{2}}\left[\begin{pmatrix} 1 \\ 0 \\ 0 \end{pmatrix}^{q} \otimes \begin{pmatrix} 1 \\ 0 \\ 0 \end{pmatrix}^{\bar{q}} - \begin{pmatrix} 0 \\ 1 \\ 0 \end{pmatrix}^{q} \otimes \begin{pmatrix} 0 \\ 1 \\ 0 \end{pmatrix}^{\bar{q}} \right] \tag{5.9}$$

and

$$\begin{aligned} |r\bar{r} + b\bar{b} - 2g\bar{g}\rangle = \frac{1}{\sqrt{6}}\Bigg[& \begin{pmatrix} 1 \\ 0 \\ 0 \end{pmatrix}^{q} \otimes \begin{pmatrix} 1 \\ 0 \\ 0 \end{pmatrix}^{\bar{q}} + \begin{pmatrix} 0 \\ 1 \\ 0 \end{pmatrix}^{q} \otimes \begin{pmatrix} 0 \\ 1 \\ 0 \end{pmatrix}^{\bar{q}} \\ & - 2 \begin{pmatrix} 0 \\ 0 \\ 1 \end{pmatrix}^{q} \otimes \begin{pmatrix} 0 \\ 0 \\ 1 \end{pmatrix}^{\bar{q}} \Bigg]. \end{aligned} \tag{5.10}$$

Using Eq. (5.9) and (5.10) in conjunction with Eq. (5.5),(5.1) and (5.6), we get the color part of transition probability as

$$\langle r\bar{r} - b\bar{b}|\mathcal{H}_{int}|\psi_{singlet}\rangle = \frac{1}{\sqrt{6}}(A_0^r - A_0^b) \quad \text{and} \tag{5.11a}$$

$$\langle r\bar{r} + b\bar{b} - 2g\bar{g}|\mathcal{H}_{int}|\psi_{singlet}\rangle = \frac{1}{\sqrt{18}}(A_0^r + A_0^b - 2A_0^g),, \tag{5.11b}$$

where, $A_0^r,\ A_0^b$ and A_0^g are the diagonal components of the matrix $A_0'(z_1') - A_0'(z_2')$. Eq. (5.11a) and (5.11b) are the effective interactions that lead to the excitations of incoming J/ψ (in the color singlet state of $c\bar{c}$) to the corresponding octet state. Due

to repulsive Coulombic interaction of q and $\bar{q}$ in the octet representation, one may expect that J/ψ may disintegrate while traversing through a $Z(3)$ wall purely by color excitation. However, we will see in the next section that this is not so and one needs to also consider spatial excitation of J/ψ due to $Z(3)$ wall.

5.1.2 Spatial excitations of J/ψ

We now consider the spatial excitations. The spatial part of the states is decided by the potential between $c\bar{c}$ in J/ψ which is taken as,

$$V\left(|\vec{r}_1 - \vec{r}_2|\right) = -\frac{\alpha_s C_F}{|\vec{r}_1 - \vec{r}_2|} + C_{cnf}\ \sigma|\vec{r}_1 - \vec{r}_2|, \tag{5.12}$$

where α_s is the strong coupling constant and σ is the string tension. For J/ψ, we will use charm quark mass $m_c = 1.28$ GeV, $\alpha_s = \pi/12$, and $\sigma = 0.16\ GeV^2$ [72, 73]. C_F is the color factor depending on the representation of the $c\bar{c}$ state. $C_F = 4/3$ for singlet state, while $C_F = -1/6$ for the octet states showing the repulsive nature of the Coulombic part of the interaction for the octet states. C_{cnf} denotes the representation dependence of the confining part of the potential. For general sources, this factor follows Casimir scaling [74, 75] for the string tension. For J/ψ in color singlet representation, $C_{cnf} = 1$ with the value of σ used here [72, 73]. It is not clear what should be the value of C_{cnf} if $c\bar{c}$ are in the octet representation. As the Coulombic part of the potential is repulsive for the octet state of $c\bar{c}$ (with $C_F = -1/6$), it is not clear if there should be a confining part of the potential at all in this case for large distances. Early lattice simulations had indicated some possibility of mildly rising potential for the confining part for $q\bar{q}$ in octet representation [76]. However, recent simulations do not show any such possibility. At large distances, the net potential between a q and $\bar{q}$ in color octet state appears to be independent of distance [77]. With the repulsive Coulombic part, this implies a very small value for C_{cnf} for the confining part. For our purpose it suffices to assume that in the octet representation, J/ψ becomes unbound, having repulsive interaction at short distances.

We have seen above that the form of A_0 in Eq.5.5 only allows for transition from color singlet to two of the color octet states given in Eqs.5.9,5.10. As we discussed

above, $c\bar{c}$ in color octet state is unbound. Thus our task should be to consider transition from initial color singlet J/ψ to unbound state of $c\bar{c}$, say in plane waves. However, this also does not look correct as the initial J/ψ (in the color singlet state) transforms to a color octet state only as it traverses the $Z(3)$ wall (as coefficients a and b in Eq.5.5 undergo spatial variations). Thus during the early part of the passage of J/ψ through the wall, it should be dominantly in the singlet state (which is a bound state) and it will be incorrect to consider transition to unbound, plane wave states of $c\bar{c}$ at this stage. Only at later stages, when the octet component is dominant, it may be appropriate to consider repulsive potential in Eq. 5.12, and unbound $c\bar{c}$ states for the transition probability. This means that the perturbation term should appropriately account for the growth of octet component for the potential in Eq. 5.12, along with a continuing singlet component with corresponding singlet potential in Eq. 5.12. This clearly is a complex issue, and a proper account of appropriate potential for this type of evolution of J/ψ cannot be carried out in simple approximation scheme considered here. We make a simplifying assumption that J/ψ becomes unbound only when it transforms to the octet representation *after* its interaction with the $Z(3)$ wall. Until then it is assumed to be in the color singlet representation. Thus, in the calculations of the spatial excitation of the J/ψ state below, we use the $c\bar{c}$ potential (Eq. 5.12) in the color singlet representation. The underlying physics is that incoming J/ψ is in the color singlet state, it interacts with Z(3) wall which excites it to higher state (spatial excitation), still in color singlet state. While traversing the Z(3) wall, and undergoing this spatial excitation, the J/ψ state also transforms to color octet state. The final state, after traversing the Z(3) wall, is spatially excited state in color octet representation, and our calculations give probability for this final state. This final octet state is unbound and hence such excited J/ψ disintegrates. We emphasize that at this stage, our aim is to point out the new possibilities of disintegration of J/ψ with Z(3) walls and this simplifying assumption should not affect our qualitative considerations and approximate estimates. We hope to give a more complete treatment in future. Thus, we continue to use the color singlet potential in Eq. 5.12, while considering the spatial excitation of J/ψ.

Since the potential is central, we perform coordinate transformations

$$\vec{R}_{cm} = \frac{\vec{r}_1 + \vec{r}_2}{2} \qquad \text{and} \qquad \vec{r} = \vec{r}_1 - \vec{r}_2, \tag{5.13}$$

where, $\vec{r}$ is the relative coordinate between q and $\bar{q}$. $\vec{R}_{cm}$ is the center of mass of J/ψ. Using Eq. (5.13) with Eq. (5.1), we get

$$A_0^r = \gamma A_0^{11}\big[\gamma(z_1' + vt')\big] - \gamma A_0^{11}\big[\gamma(-z_2' + vt')\big]. \tag{5.14}$$

z_1' and z_2' are written in terms of $\vec{R}_{cm}$ and $\vec{r}$. Similar expressions can be obtained for A_0^b and A_0^g. In the above coordinates, the J/ψ wave function is $\Psi(\vec{R}_{cm})\psi(\vec{r})$. For simplicity, we assume that the center of mass motion remains unaffected by the external perturbation. Then $\Psi(\vec{R}_{cm})$ has the plain wave solution, while $\psi(\vec{r})$ can be written $\psi(r,\theta,\phi) = \psi(r)Y_l^m(\cos\theta,\phi)$. As J/ψ is the $l = 0$ state, we have

$$\psi_i = \psi(r)Y_0^0 \qquad \text{and} \quad \psi_j = \psi_n(r)\,Y_l^m(\cos\theta,\phi)\,. \tag{5.15}$$

The radial part, $\psi(r)$, is obtained by solving radial part of Schrödinger equation with effective potential given by

$$V(r) = -\frac{\alpha_s C_F}{r} + C_{cnf}\ \sigma r + \frac{l(l+1)}{2\mu r^2}, \tag{5.16}$$

where μ is the reduced mass. When we use Eq. (5.11), (5.14) and (5.15) in Eq. (5.3), we get one of the terms as

$$\int_{-\infty}^{\infty} \psi_j^* A_0^r \psi_i\ d\vec{r}_1 d\vec{r}_2 = \int_0^{\infty}\int_{-1}^{1}\int_0^{2\pi} \psi_n^*(r)Y_l^{m*}(\cos\theta,\phi)\,A_0^r\ Y_0^0\psi_{100}(r)\ r^2\ dr d(\cos\theta)d\phi. \tag{5.17}$$

In the above equation, we have ignored the motion of the center of mass of charmonium and have considered only the relative coordinate. Under $\cos\theta \to -\cos\theta$, $A_0^r \to -A_0^r$ and ψ_i does not change. So if $Y_l^m(\cos\theta,\phi) = Y_l^m(-\cos\theta,\phi)$ then RHS of Eq. (5.17) is zero. Thus we do not get any transition to a state which is symmetric under $\cos\theta \to -\cos\theta$. This has very important significance. While the color part prohibits the transition to singlet final states, the space dependence of interaction forbids the transition to the $l = 0$ state (in color octet). Thus we see that purely color excitation

of J/ψ due to A_0 field of a domain wall is not possible. The excitation is possible to the first excited state of an octet (like an 'octet χ' state). As the excited state will have a radius larger than the $l = 0$ state it is more prone to melting in the medium, (though with color octet composition, the final state becomes unbound anyway).

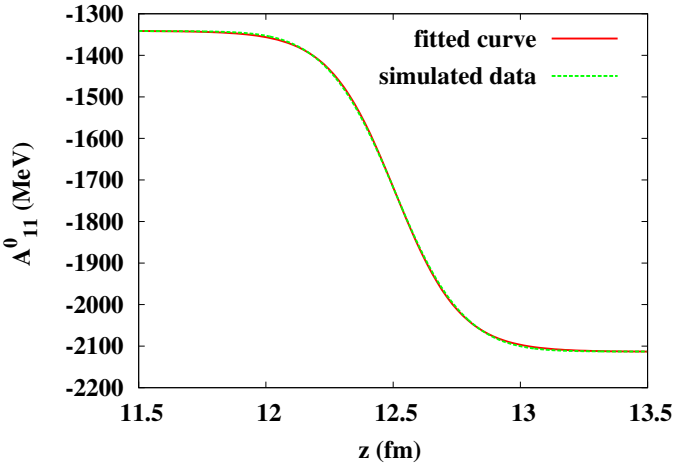

Figure 5.1: A_0 profile across the Z(3) domain wall for $T = 400$ MeV. Only $(1, 1)$ component is shown. Other components are similar. See ref. [30] for details. This is same as Fig. 2.6. We show it here for the sake of completeness.

5.2 Results

We numerically compute the integral given in Eq. (5.3) with various parameters given after Eq. 5.12. The profile of A_0 is calculated from the profile of the Polyakov loop order parameter for a Z(3) domain wall at a temperature T =400 MeV (as a sample value). The details of this are given in ref. [30]. As explained there, the resulting profile is very well fitted by the functional form $p\tanh(qx + r) + s$, see Fig. 5.1. This is same as Fig. 2.6. We show it here again for the convenience of the reader.

We calculated the wave functions for various states of $c\bar{c}$ with the complete potential given by Eq. (5.16). For the calculation of the wave-functions for various states of $c\bar{c}$ we have used Numerov method for solving the Schrödinger equation. We have also used energy minimization technique to get the wave functions and the bound state energy and the results obtained by both the methods match very well. Fig. (5.2)

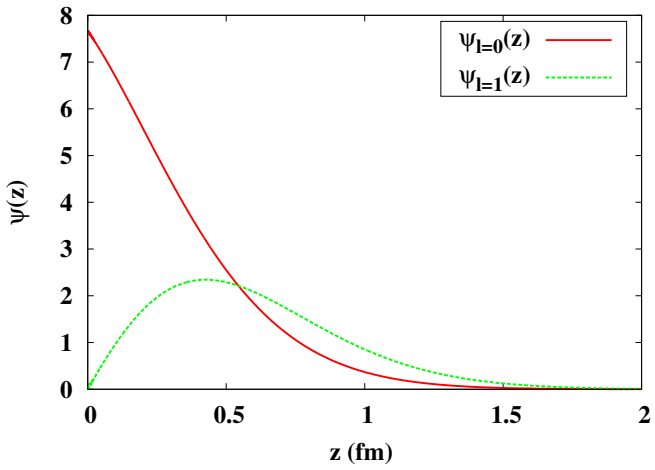

Figure 5.2: (Color online) Wave functions for J/ψ ($l = 0$) and χ ($l = 1$) states.

shows the radial part of the wave function for the $l = 0, 1$ states of charmonium. The bound state contributions to the energy (excluding the rest mass of quarks) are found to be $E_0 = 0.447$ GeV for J/ψ and $E_0 = 0.803$ GeV for χ state ($l = 1$). We see from Fig.2 that the radius of J/ψ is about 0.5 fm while that for χ is about 0.8 fm. Debye length in QGP at $T = 200$ MeV is $r_d \sim 0.6$ fm and smaller at higher temperatures. Thus χ state is unstable and it should melt easily in the medium (apart from the fact that in color octet state it also becomes unbound). Fig.3 shows the combined probability of transition to both the color octet χ states (Eqs.5.9,5.10) for an incoming J/ψ with different velocities moving normal to the domain wall. As we see, the probability rapidly rises as a function of velocity. However, for large velocities the probability of transition becomes large making first order perturbation approximation insufficient, and one needs more reliable estimates. Thus, the plot in Fig.3 should be trusted only for small velocities. Nonetheless, the trend at higher velocities strongly suggests that most of J/ψ will disintegrate while interacting with $Z(3)$ walls.

5.3 Conclusions

These results show that on interaction with a $Z(3)$ domain wall, a J/ψ particle will make an excitation to a higher orbital state in color octet representation which is unbound and will readily melt in the surrounding QGP medium. At higher energies,

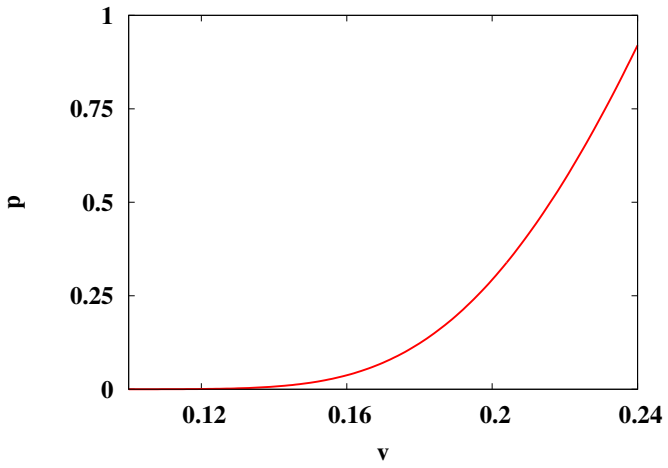

Figure 5.3: Probability p of transition of J/ψ to color octet χ states vs. its velocity v. Note that the probability rapidly rises with v.

the transition probability keeps increasing, making the first order perturbation theory inapplicable and the results are not trustworthy. Nonetheless, this implies that at higher energies, almost all J/ψ are expected to disintegrate in this manner. This strong P_T dependence of J/ψ disintegration probability is a distinctive signature of our model wherein the probability of disintegration of J/ψ is enhanced with higher P_T. This can be used to distinguish this mechanism from the conventional Debey screening suppression. A very crucial point in the entire discussion is the Debye screening of the A_0 profile of the domain wall itself as it carries color. At temperature 400 MeV, the domain wall has a thickness of $\sim 1.5\ fm$ and the Debye radius for QGP is $\sim 0.7\ fm$. This means that Debye screening will be effective outside a sphere of diameter $\sim 1.5\ fm$. So we do not expect the domain wall to be significantly Debye screened. In the above discussion, we have completely ignored the effects of a thermal bath (QGP medium) on the potential (Eq. 5.12) between $c\bar{c}$ ([72, 78]). However as these effects make the potential between $c\bar{c}$ weaker, the charmonium state *swells*. So it will be even easier for the interaction to break these bound states. These temperature effects will also be crucial for other heavier $q\bar{q}$ states like bottomonium as they have large binding energies. Another important aspect which has been ignored for the sake of simplicity, in the above calculations, is the question of the center of mass motion. This assumption is correct only in an average sense as the average force

$(\Delta V/\Delta z)$ acting on c and $\bar{c}$ vanishes. This averaging is done over the thickness Δz, which is the thickness of the domain wall itself. However as the instantaneous force $(\partial V/\partial z)$ is non-zero, there is a non-zero instantaneous acceleration of the center of mass. A more detailed analysis of the problem is required to incorporate all these details. One also needs to include the effects of dynamical quarks leading to explicit breaking of Z(3) symmetry. We mention that such a disintegration of J/ψ from a color electric field may not necessarily come from a background domain wall arising in QGP medium. In a thermal medium there are always statistical fluctuations. These gluonic fluctuations will have energy of order $\sim T$. Depending on the correlation length of the fluctuation, a J/ψ passing through it may disintegrate via the mechanism discussed above. It would be interesting to study the effect of these thermal gluonic fluctuations on the spectrum of mesons.

Chapter 6

Disintegration of quarkonia in Heavy Ion Collisions due to non-trivial profile of the Polyakov loop of $Z(3)$ interfaces

In the last chapter we have discussed the implications of CP violating effects of gauge potential A_0 associated with a $Z(3)$ domain wall. There we have proposed a novel mechanism for disintegration of quarkonia due to this CP violation from $Z(3)$ walls [71]. We discussed certain important issues of gauge choice and the color dependence of the A_0 profile associated with the $Z(3)$ walls. In view of these discussions it becomes important to study whether quarkonia disintegration due to the $Z(3)$ domain walls essentially requires such CP violating interaction. We consider this issue in this chapter. We show that quarkonia disintegration due to the $Z(3)$ domain walls can occur solely due to spatial variation of $l(x)$ profile of the $Z(3)$ wall, even in the absence of CP violating interaction arising from the associated A_0 profile. For this we consider the interaction of q and $\bar{q}$ with the $Z(3)$ wall, as in ref. [79], where the interaction is modeled in terms of an effective quark mass depending on the value of $|l(x)|$. We find that quarkonia on interaction with a $Z(3)$ wall again has non-zero probability of getting excited to higher states. This happens because q and $\bar{q}$ interact with $Z(3)$ walls at different space-time points which leads to the excitation of quarkonia to

higher excited states, which are short lived in the QGP medium.

6.1 Interaction of quarkonia with Z(3) walls with effective quark mass

Like Polyakov loop order parameter, the effective quark mass is also different in the confined and the deconfined phases of QCD. While in the QGP phase (where $l(x)$ assumes a non-zero value) quarks are supposed to have the current masses, in the confined phase (where $l(x) = 0$) quarks are supposed to acquire constituent mass of order 300 MeV. This indicates a possible dependence of effective quark mass on the magnitude of Polyakov loop order parameter. Hence we model the dependence of effective mass of the quarks on the Polyakov loop order parameter, and study the interaction of quarkonia with $Z(3)$ interfaces. We show that this interaction (treated as a time dependent perturbation for a quarkonia traversing through a $Z(3)$ wall) disintegrates quarkonia by exciting it to higher states of $q\bar{q}$ system which are supposed to be short-lived in the QGP medium. The effective mass can be modeled as in ref. [80] identifying $l(x)$ with the color dielectric field χ, where effective mass of the quark is inversely proportional to χ. This leads to divergent quark mass in the confining phase, consistent with the notion of confinement. However we know that the divergence of quark energy in the confining phase should be a volume divergence (effectively the length of string connecting the quark to the boundary of the volume). $1/l(x)$ dependence will not have this feature, hence we do not follow this modeling. Further, in the spirit of the expectation that a linear term in l should arise from explicit symmetry breaking due to dynamical quarks [20, 22–24] and also for the sake of simplicity, we use the modeling of the quark mass dependence on $l(x)$ in the following manner [79].

$$m(x) = m_q + m_0(l_0 - |l(x)|) \tag{6.1}$$

Here $l(x)$ represents the profile of the $Z(3)$ interface, and l_0 is the vacuum value of $|l(x)|$ appropriate for the temperature under consideration. m_q is the current quark mass as appropriate for the QGP phase with $|l(x)| = l_0$, with $m_u \simeq m_d = 10$ MeV,

$m_s = 140$ MeV, $m_c = 1.28$ GeV and $m_b = 4.66$ GeV. m_0 characterizes the constituent mass contribution for the quark. We will take $m_0 = 300$ MeV. Note that here $m(x)$ remains finite even in the confining phase with $l(x) = 0$. As mentioned above, this is reasonable since we are dealing with a situation where $l(x)$ differs from l_0 only in a region of thickness of order 1 fm, thickness of the $Z(3)$ domain wall. (We mention that we continue to neglect the effect of dynamical quark in the consideration of the profile of $Z(3)$ which will arise from a linear term in l in the effective potential of $l(x)$). Such a linear term leads to slightly *asymmetric* profile of $l(x)$ which does not affect main considerations presented below.)

We work in the rest frame of the quarkonia and consider the domain wall coming and hitting the quarkonia with a velocity v along the z-axis. Considering the space dependent part of $m(z)$ in Eq.6.1 as a potential term in the Dirac equation for the propagation of quarks and antiquarks, one can write the interaction of the quarkonia with the wall as,

$$\mathcal{H}_{int} = m^q(z_1) + m^{\bar{q}}(z_2) \tag{6.2a}$$

$$\text{with, } m^q(z) = m^{\bar{q}}(z) = m_0(l_0 - |l(z)|) \tag{6.2b}$$

where z_1 and z_2 are the coordinates of q and $\bar{q}$ in quarkonia. (Thus, note that quark and antiquark have the same interaction with the $Z(3)$ wall in complete contrast to the CP violating case of the previous chapter. As we mentioned above, here the excitation of quarkonia occurs due to different space-time locations of the quark and the antiquark during propagation of the quarkonia through the $Z(3)$ wall.)

We use first order time dependent perturbation theory to study the excitation of quarkonia due to the background $l(x)$ profile and consider the transition of quarkonia from initial energy eigenstate ψ_i with energy E_i to the final state ψ_j with energy E_j. The transition amplitude is given by

$$\mathcal{A}_{ij} = \delta_{ij} - \ i \int_{t_i}^{t_f} \langle \psi_j | \mathcal{H}_{int} | \psi_i . \rangle e^{-i(E_j - E_i)t} dt. \tag{6.3}$$

The states are determined using the potential between $q\bar{q}$ in quarkonia taken is

$$V\left(|\vec{r}_1 - \vec{r}_2|\right) = -\frac{\alpha}{|\vec{r}_1 - \vec{r}_2|} + \sigma |\vec{r}_1 - \vec{r}_2| \tag{6.4}$$

where r_1 and r_2 are the coordinates of the quarks and antiquarks respectively, σ is the string tension, $\alpha = \frac{4}{3}\alpha_s$ and α_s is the strong coupling constant. Since the potential is

central, we perform coordinate transformations

$$\vec{R}_{cm} = \frac{\vec{r}_1 + \vec{r}_2}{2} \qquad \text{and} \qquad \vec{r} = \vec{r}_1 - \vec{r}_2, \tag{6.5}$$

where, $\vec{r}$ is the relative coordinate between q and $\bar{q}$. $\vec{R}_{cm}$ is the center of mass of quarkonia. Hence, $z_1 = R_{cm} + \frac{r}{2}\cos\theta$ and $z_2 = R_{cm} - \frac{r}{2}\cos\theta$. And, one can write the quarkonia wave function as $\Psi(\vec{R}_{cm})\psi(\vec{r})$. To simplify the calculation, we assume that the center of mass motion remains unaffected by the external perturbation. As a result $\Psi(\vec{R}_{cm})$ has the plain wave solution, and $\psi(\vec{r})$ can be written $\psi(r,\theta,\phi) = \psi(r)Y_l^m(\cos\theta,\phi)$. As we are considering transition form ground state to other states of quarkonia, we have

$$\psi_i = \psi(r)Y_0^0 \qquad \text{and} \quad \psi_j = \psi_n(r)\,Y_l^m(\cos\theta,\phi)\,. \tag{6.6}$$

The radial part, $\psi(r)$, is obtained by solving radial part of the Schrödinger equation (for heavy quarkonia, non-relativistic treatment is adequate) with the effective potential given by

$$V_r(r) = -\frac{\alpha_s}{r} + \sigma r + \frac{l(l+1)}{2\mu r^2} \tag{6.7}$$

where μ is the reduced mass. Using Eqn. 6.2 and 6.6 one can find

$$\begin{aligned}\langle\psi_j|\mathcal{H}_{int}|\psi_i\rangle = \int_0^\infty \int_{-1}^1 \int_0^{2\pi} & \psi_n^*(r)Y_l^{m*}(\cos\theta,\phi) \\ & \{m^q\big[\gamma(z_1' + vt')\big] + m^{\bar{q}}\big[\gamma(-z_2' + vt')\big]\} \\ & Y_0^0\psi_{100}(r)\; r^2\; dr d(\cos\theta) d\phi.\end{aligned} \tag{6.8}$$

We again emphasize that in the above equation, we have ignored the acceleration of the center of mass of quarkonia and have considered only the relative coordinate. Here functions m^q, $m^{\bar{q}}$ and ψ_i's are symmetric under $\cos\theta \to -\cos\theta$. So if $Y_l^m(\cos\theta,\phi) = -Y_l^m(-\cos\theta,\phi)$ then RHS of Eqn. (6.8) is zero. Thus we do not get any transition to a state which is not symmetric under $\cos\theta \to -\cos\theta$.

6.2 Results

We numerically compute the integral given in Eqn. (6.3) with various parameters for J/ψ and for Υ states. We have calculated the wave functions for various states

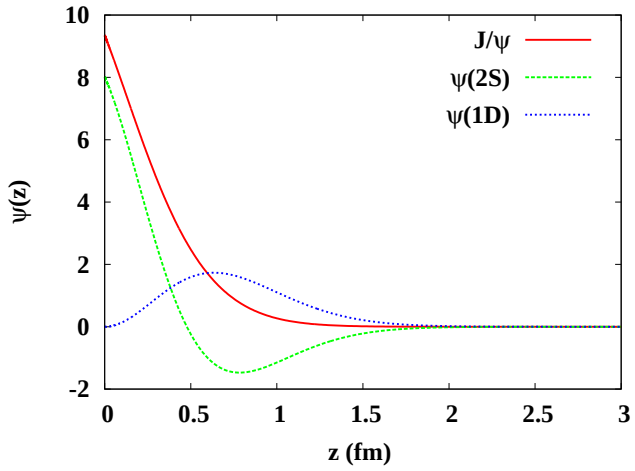

Figure 6.1: Radial part of wave functions for different states of $c\bar{c}$.

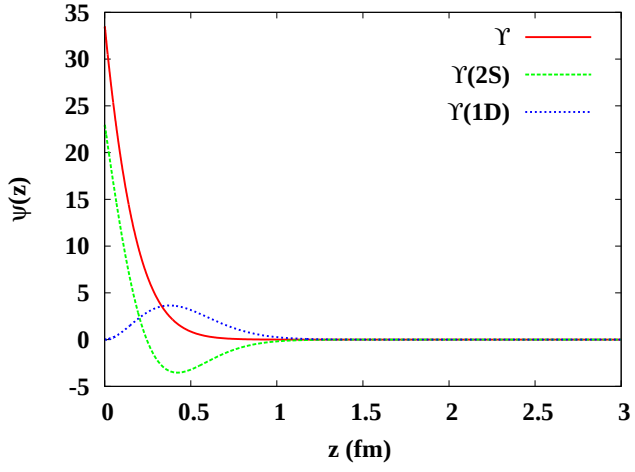

Figure 6.2: Radial part of wave functions for different states of $b\bar{b}$.

of $q\bar{q}$ with the complete potential given by Eqn. (6.7). For the calculation of the wave-functions for various states of $q\bar{q}$ we have used Numerov method for solving the Schrödinger equation. As we want to show the different possible mechanism for quarkonia disintegration with order of magnitude estimate, so we have taken same α and σ for $c\bar{c}$ and $b\bar{b}$ bound state which are $\alpha = 0.471$ and $\sigma = 0.192\ GeV^2$ [59]. Fig. (6.1) and (6.2) shows the radial part of the wave function for different states of charmonium and bottomonium respectively.

As no higher excited state of charmonium is expected to be stable in the QGP medium other than J/ψ even at $T = 200$ MeV, J/ψ will dissociate in medium on interaction with domain wall if it makes transition to excited states of charmonium. Fig. (6.3) shows the probability of transition of J/ψ to other excited states of charmonium for different velocity of the charmonium (consequently, of the wall in the charmonimum rest frame) on interaction with the domain wall at $T = 400$ MeV. Transition probability is very small for small velocity, it increases with velocity and attains a maximum value $\simeq 11\%$ and again decreases to very small value for very high speed of J/ψ hitting the domain wall perpendicularly. The maximum probability is smaller (less than 2%) for domain wall at $T = 200$ MeV. Similarly at $T = 400$ MeV only Υ is bound and all other states of bottomonium are unbound. So Υ will dissociate in medium by the same mechanism if it makes transition to excited states. Fig. (6.4) shows the probability of transition from Υ to other excited states of bottomonium for different velocity on interaction with domain wall at $T = 400$ MeV. The behavior of the plot of the probability of transition vs. velocity is same as for the case of J/ψ. The difference is in the maximum value of the probability and the corresponding value of the temperature. Transition probability is negligible (less than 1%) for domain wall at $T = 200$ MeV.

6.3 Conclusions

These results conclusively show that on interaction with a $Z(3)$ domain wall, a J/ψ or Υ will make an excitation to higher orbital states which will readily melt in the surrounding QGP medium. Transition probability first increases with energy and

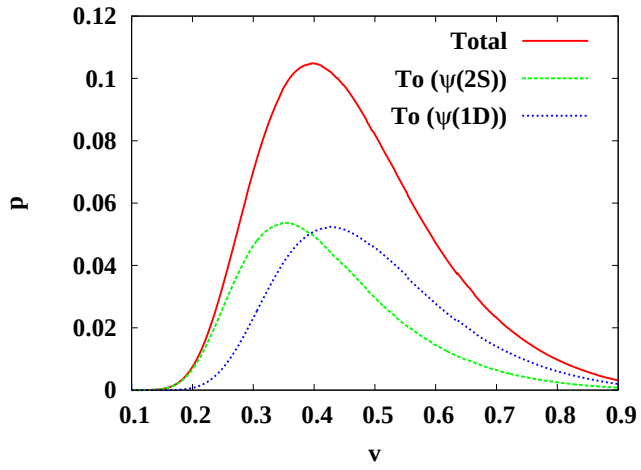

Figure 6.3: Probability p of transition from J/ψ to different excited states of charmonium vs. its velocity

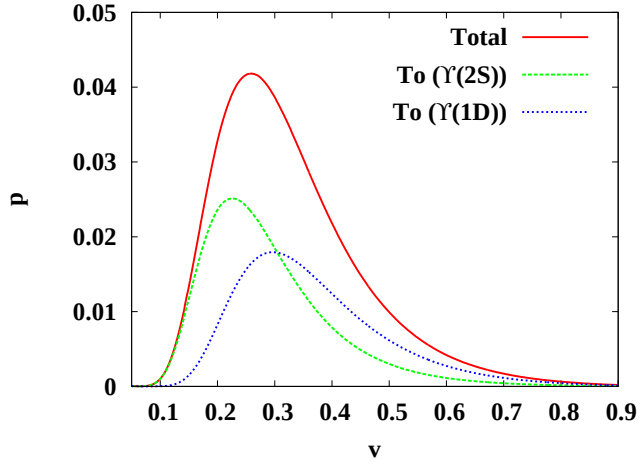

Figure 6.4: Probability p of transition from Υ to different excited states of bottomonium vs. its velocity

again decreases to very small value. For very small velocity the results are not trustworthy as we have neglected the acceleration of center of mass. Nonetheless, this implies that at some energies the suppression will increase in this manner, decreasing subsequently at higher energies. This new type of P_T dependence of quarkonia disintegration probability is a distinctive signature of our model. This can be used to distinguish this mechanism from the conventional Debye screening suppression.

We mention again that the results in this chapter show that quarkonia disintegration due to the $Z(3)$ domain walls can occur solely due to spatial variation of $l(x)$ profile of the $Z(3)$ wall, even in the absence of CP violating interaction arising from the associated A_0 profile (as was discussed in chapter 5). It thus becomes interesting to investigate both these effects together on quarkonia disintegration. $l(x)$ profile will affect the quark and the antiquark in the same manner while the A_0 profile will lead to the CP violating interaction, distinguishing quark from antiquark. We hope to investigate this in a future work.

Note that for the case of thermal quarkonia, thermal effects make the potential between $q\bar{q}$ weaker, leading to *swelling* of quarkonia states. This implies that it will be easier for the interaction to break these bound states when finite temperature effects are incorporated in the quark-antiquark potential. Another important aspect which has been ignored for the sake of simplicity in our calculations is the question of the acceleration of center of mass. This assumption is correct only for large velocities. A more detailed analysis of the problem is required to incorporate all these details. One also needs to include the effects of dynamical quarks leading to explicit breaking of $Z(3)$ symmetry (consequently asymmetric profile of $l(x)$ for a $Z(3)$ wall).

Chapter 7

Quarkonia Disintegration due to time dependence of the $q\bar{q}$ potential in Relativistic Heavy Ion Collisions

In the last two chapter we have discussed dissociation of quarkonia on interaction with $Z(3)$ walls which appear as topological defects due to spontaneous breaking of $Z(3)$ symmetry in QGP. Here we will consider other possibilities of quarkonia melting [81] due to time dependence of the $q\bar{q}$ potential, without invoking any such exotic objects.

The conventional mechanism of quarkonia disassociation becomes effective when the medium thermalizes, potential between $q\bar{q}$ gets Debye screened resulting in the swelling of quarkonia. If the Debye screening length of the medium is less than the radius of quarkonia, then $q\bar{q}$ may not form bound states, leading to melting of the initial quarkonium. Due to this melting, the yield of quarkonia will be *suppressed*. In the above picture, suppression of quarkonia occurs when the temperature of QGP achieves a certain value, T_D, so that the Debye screening melts the quarkonium bound state. Thus, if the temperature remains smaller than T_D, so that Debye screening length remains larger than the quarkonia size, no suppression is expected. This type of picture is consistent with the *adiabatic* evolution of a quantum state under changing potential. Original quarkonia has a wave function appropriate for zero temperature potential between a q and $\bar{q}$. If the environment of the quarkonium changes to a finite temperature QGP adiabatically, with Debye screened potential, the final state will

evolve to the quarkonium state corresponding to the finite temperature potential. If temperature remains below T_D, quarkonium wave function changes (adiabatically) but it survives as the quarkonium.

We question this assumption of adiabatic evolution during the thermalization stage for ultra-relativistic heavy-ion collisions, such as at RHIC, and especially at LHC. In the next section we will discuss the validity of adiabaticity for ultra relativistic heavy ion collisions, especially during the thermalization stage.

7.1 Validity of Adiabaticity for Ultra Relativistic Heavy Ion Collisions

At very high energy it is possible that thermalization is achieved in a very short time, about 0.25 fm for RHIC and even smaller about 0.1 fm for LHC [31]. The issue of thermalization in RHICE has been extensively investigated using different approaches for the pre-equilibrium stages. Ads/CFT correspondence has also been utilized to give and upper bound on the thermalization time scale of $1/T$ [82], leading to a time scale of 0.4 fm for $T = 500$ MeV. Estimates based on color glass condensate model give values of thermalization time ranging up to about 1 fm., see refs. [83, 84] One can take a conservative estimate of the thermalization time scale to be less than 1 fm as suggested by the elliptic flow measurements [43]. For J/ψ and even for Υ, typical time scale of $q\bar{q}$ dynamics will be at least 1-2 fm from the size of the bound state and the fact that $q\bar{q}$ have non-relativistic velocities. Also, ΔE between J/ψ and its next excited state (χ) is about 300 MeV (400 MeV for Υ states), leading to transition time scale ~ 0.7 fm (0.5 fm for Υ). Thus the change in the potential between q and $\bar{q}$ occurs in a time scale which is at most of the same order, and likely much shorter than, the typical time scale of the dynamics of the $q\bar{q}$ system, or the time scale of transition between relevant states. We have shown in section 4.31 that required condition for validity of adiabatic approximation is the opposite, that means the time scale for thermalization should be much larger than the time scale corresponding to energy gap between nearest energy level. The problem, therefore, should be treated in terms of a time dependent perturbation and survival probability

of quarkonia should be calculated under this perturbation. It is immediately clear that even if the final temperature remains less than T_D, if the change in potential is fast enough invalidating the adiabatic assumption, then transition of initial quarkonium state to other excited states will occur. Such excited states will have much larger size, typically larger than the Debye screening length, and will melt away. Thus quarkonia melting can occur even when QGP temperature remains below T_D. We mention that adiabatic evolution of quarkonia states has been discussed earlier for the *cooling stage* of QGP in relativistic heavy ion collisions in the context of sequential suppression of quarkonia states [85, 86]. However, as far as we are aware, validity of adiabatic evolution during the *thermalization* stage has not been discussed earlier.

7.2 Quarkonia Evolution Using Sudden Approximation

Given the large difference between thermalization time scale of order 0.1 - 0.2 fm [31], and the time scale of $q\bar{q}$ dynamics in a quarkonium bound state being of order 1-2 fm (or the time scale of transition between relevant states being 0.5 - 0.7 fm), it may be reasonable to use the *sudden* perturbation approximation. The initial wave function of the quarkonium cannot change under this sudden perturbation. Thus, as soon as thermalization is achieved with QGP temperature being T_0 (which may remain less than T_D for the quarkonium state under consideration), the initial quarkonium wave function is no longer an energy eigen state of the new Hamiltonian with the $q\bar{q}$ potential corresponding to temperature T_0. One can find overlap with the new eigen states, giving us the survival probability of the quarkonium as well as the probability of its transition to other excited states. We will follow the sudden approximation to calculate the survival probability of quarkonia. We will also estimate the error in using this approximation with the knowledge that the time scale of thermalization is non-zero, though small (less than 1 fm). We mention here that the sudden approximation has been used earlier in the context of heavy-ion collisions for production of hydrogen like atoms at late stages of the evolution of the system, see ref. [87].

For calculating the zero temperature wave function of the quarkonium we use the

following potential between q and $\bar{q}$.

$$V(r) = -\frac{\alpha}{r} + \sigma r \tag{7.1}$$

where $\alpha = \frac{4}{3}\alpha_s$, α_s is the strong coupling constant, and σ is the string tension. For J/ψ, we will use charm quark mass $m_c = 1.28$ GeV, $\alpha = 0.471$, and $\sigma = 0.192\ GeV^2$ [59]. For Υ, we use the bottom quark mass $m_b = 4.66$ GeV.

For calculating wave functions at finite temperature we use the following potential which incorporates Debye screening

$$V(r) = -\frac{\alpha}{r} exp(-\omega_D r) + \frac{\sigma}{\omega_D}(1 - exp(-\omega_D r)) \tag{7.2}$$

where $\omega_D = gT\sqrt{1 + N_f/6}$ [59]. We use $N_f = 3$. We have calculated wave functions for charmonium and bottomonium states at different temperatures with above potentials using Numerov method for solving the Schrödinger equation. We have also used energy minimization technique to get the wave functions for the ground states and the binding energy and the results obtained by both the methods match very well. Fig.7.1 shows plots of wave functions for J/ψ at $T = 0$ and 200 MeV. With finite temperature potential (Eq.7.2), excited states of charmonium are not found for $T \geq 200$ MeV. Fig.7.2 shows wave functions for Υ states at $T = 0, 200, 400$, and 500 MeV. For Bottomonium, we find excited state $\Upsilon(2S)$ at $T = 200$ MeV which is shown in Fig.7.3, along with the ground state $\Upsilon(1S)$ at $T = 0$.

As we mentioned, we use the sudden approximation to calculate the survival probability of quarkonium state which is calculated directly by calculating (mod square of) the overlap of the wave function of the zero temperature quarkonium state with the wave function of the appropriate state at finite temperature. Figs.7.1-7.3 immediately give an idea of this overlap, which is clearly decreasing with increasing temperature implying decreasing survival probability of the quarkonium. Fig.7.4 shows the plot of survival probabilities for J/ψ and for Υ as a function of temperature. Survival probabilities are plotted up to a temperature T_D beyond which the quarkonium state does not exist any more due to Debye screening in the potential in Eq.7.2. We note dramatic decrease in survival probabilities down to about 10 % as temperature increases to about 260 MeV and 590 MeV respectively for the two cases. It is important

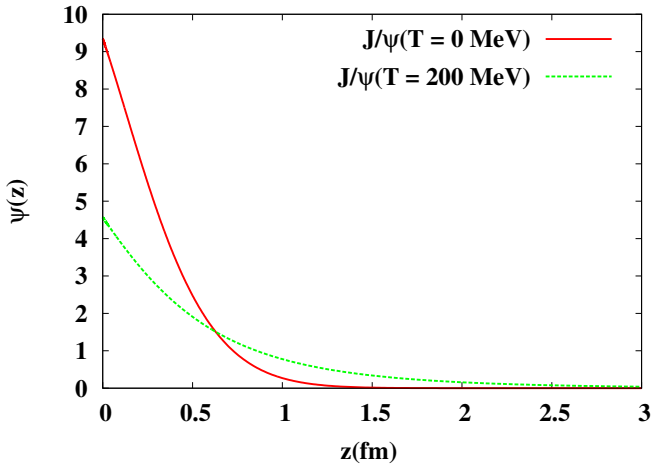

Figure 7.1: Wave functions for J/ψ states at different temperatures.

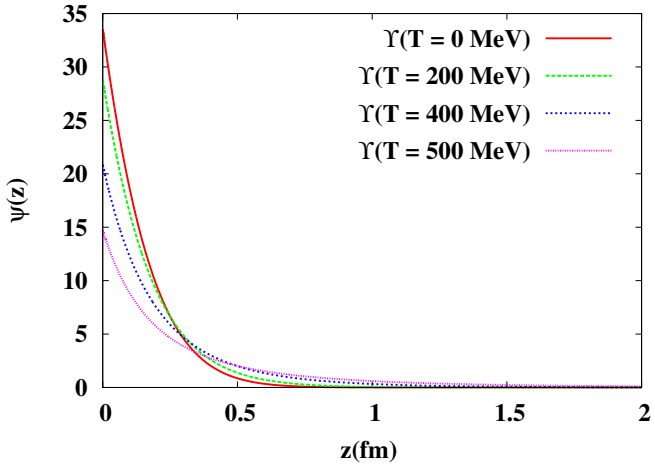

Figure 7.2: Wave functions for $\Upsilon(1S)$ states at different temperatures.

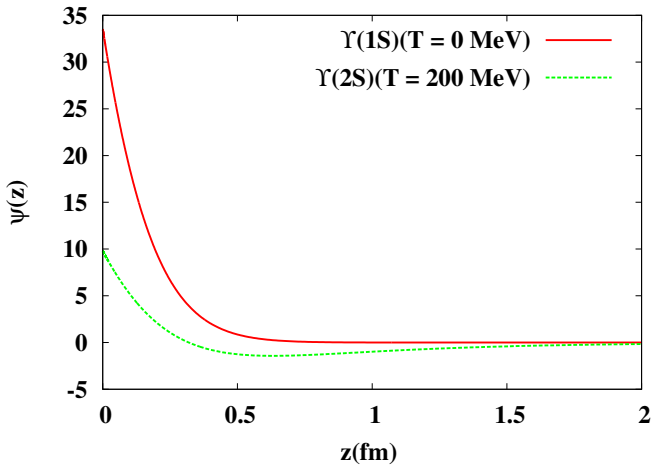

Figure 7.3: Wave functions for $\Upsilon(1S)$ and $\Upsilon(2S)$ states at $T = 0$ and $T = 200$ MeV respectively.

to note that survival probabilities for J/ψ and Υ significantly reduce even when the temperature remains smaller than T_D for the respective case. The overlap of $\Upsilon(2S)$ wave function at $T = 200$ MeV and $\Upsilon(1S)$ at $T = 0$ (Fig.7.3) gives the transition probability of an initial Υ to the excited state to be about 10 %. We now estimate

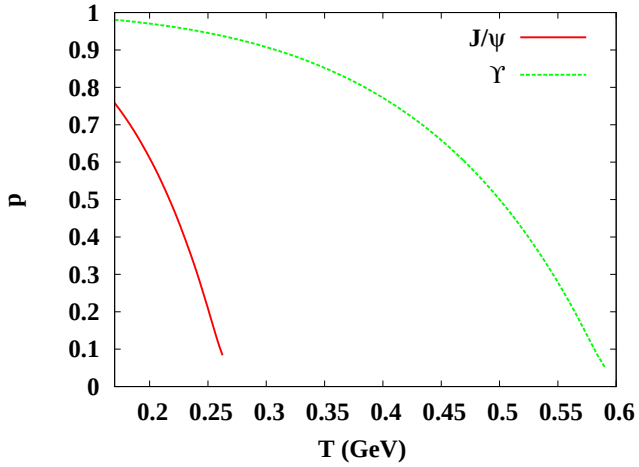

Figure 7.4: Survival probabilities of initial $T = 0$ J/ψ and Υ states in QGP at different temperatures calculated in the sudden (quench) approximation.

the error in using this sudden approximations by calculating the probability ζ of transition of the original quarkonium state to some other state during the time scale τ of

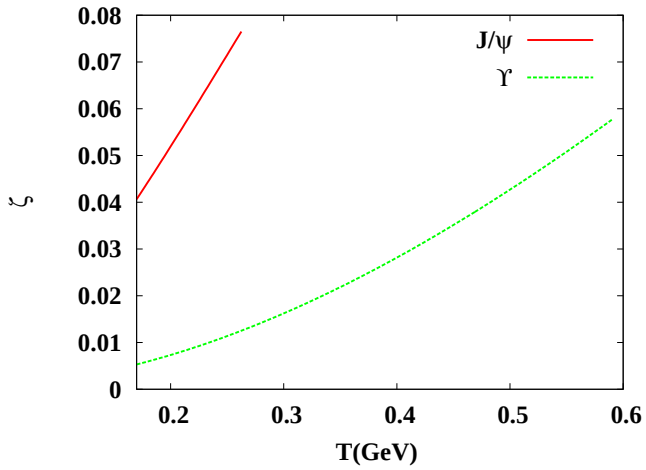

Figure 7.5: Plot of the probability ζ encoding the error in making the sudden approximation. ζ is the probability that the initial quarkonium state does not remain in the same state during the time period τ (taken as 0.5 fm here) of the change of the potential.

the change of the potential using the relations

$$\zeta = \tau^2 \Delta \bar{H}^2 \tag{7.3}$$

Here, <> denotes the expectation value in the initial quarkonium state. For calculating the time averaged Hamiltonian $\bar{H}$, we model the time dependence of the temperature in the following manner,

$$T(t) = \frac{t}{\tau} T_0 \tag{7.4}$$

where T_0 is the maximum temperature of QGP. This linear increase of temperature is a simple way to model the initial non-equilibrium stage of the parton system. A more careful calculation should account for the non-equilibrium nature of the system. However, to roughly estimate the error in making the sudden approximation, it should be reasonable to assume a quasi-equilibrium system, with initially increasing temperature upto a maximum value T_0 (which will subsequently decrease due to continued plasma expansion). In Fig.7.5 we provide plot of ζ for different quarkonia states as a function of temperature. We have taken thermalization time $\tau = 0.5$ fm for

these plots (which is on the higher side of the expected value at RHIC and at LHC). We note that the error in using sudden approximation remains less than about 8%.

7.3 Discussion

We point out the main difference between our approach and the conventional approaches for calculating heavy quarkonium suppression in QGP. In conventional approach, quarkonium suppression is calculated for a QGP medium which has achieved high enough temperature T_D so that Debye screening becomes effective in making the quarkonium unbound. If temperature remains below T_D one does not expect any suppression of the corresponding quarkonium state. Our approach is to focus on the situation when temperature remains below T_D (for the specific quarkonium under consideration). If the initial thermalization of QGP happens very slowly in time scale much larger than the time scale of quarkonium which is of order 1 fm, then indeed we will conclude that no quarkonium suppression will be expected. However, in ultra-relativistic heavy-ion collisions thermalization is definitely achieved within a time scale of about 1 fm (from elliptic flow measurements) [43], which is of same order as the dynamical scale of $q\bar{q}$ in the quarkonium bound state (or the time scale of transition between relevant states). In such a situation one cannot assume that the initial zero temperature quarkonium state will simply evolve to the finite temperature quarkonium state. Instead, time dependent perturbation theory should be used to calculate the survival probability of the initial quarkonium state. In fact expected thermalization time scale at RHIC and LHC may be as short as 0.25 - 0.1 fm respectively [31]. With such rapid thermalization, use of sudden perturbation approximation may be appropriate. We calculate survival probability of quarkonium (and transition to excited state for Υ) and show that even when temperature of QGP remains much below T_D, the quarkonium state can decay with significant probability. Even if the temperature exceeds T_D, during initial stages of heating the decay of initial quarkonium state due to time dependent potential, as discussed here, should be incorporated in calculating the final net quarkonium suppression.

It thus provides new avenues for the experiments to look for different patterns of suppression of quarkonium depending on the temperature. For the same maximum

temperature T_0, nuclear effects, the time dependent perturbation effects (as used here in sudden approximation), and the conventional Debye screening effects, all may show qualitatively different behavior when the duration of thermalization τ is changed. One way to clearly distinguish our mechanism from the conventional mechanism is to study quarkonium suppression for varying QGP temperatures and the thermalization time scale independently. One may achieve this by considering different centrality, or rapidity, or by using different combinations of nucleus size and collision energies so that the thermalization time and QGP temperature can be varied independently.

Chapter 8

Summary

In the following we present a brief summary of our work, presented in this thesis. We have discussed alternate mechanisms of quarkonia disintegration, showing that even when the temperature T remain below the Debye temperature T_D (above which the Debye length becomes smaller than the size of quarkonia), the quarkonia can melt in the medium. This is totally different than the conventional mechanism of quarkonia melting, where quarkonia will melt only when $T \geq T_D$.

We first presented a brief review of the confinement-deconfinement phase transition, where thermal expectation value of Polyakov loop $l(x)$ acts as order parameter for this phase transition. $l(x)$ vanishes in the confined phase, respecting $Z(3)$ symmetry, whereas in the deconfined phase it takes non-zero value leading to spontaneous breakdown of $Z(3)$ symmetry. This leads to three degenerate vacua corresponding to $l = 1, e^{2\pi i/3}, e^{4\pi i/3}$. After the symmetry breaking, field can choose any of the vacua in different regions of space, hence domains with different l form. The junction of different domains give rise to topological defects, in particular, $Z(3)$ walls at the junctions of two domains corresponding to different vacua. We have calculated the profile of $l(x)$ associated with the $Z(3)$ interpolating between different vacua. We have confined the discussion in this thesis to pure QCD and neglected the effect of dynamical quark in the profile of $Z(3)$ walls.

Subsequently we have calculated the background gauge field (A_0) associated with the $l(x)$ profile of the wall. This has CP violating effect on the interaction of quarks with the wall. We have showed that the CP violating interaction of this background

A_0 field leads to color excitation of quarkonia along with special excitation, which will imply quarkonia melting in the QGP medium. We have used first order time-dependent perturbation theory to calculate the transition of the initial quarkonia to excited states and we found that probability of transition increases with kinetic energy of the quarkonia.

We then address the issue whether heavy quarkonia disintegration due to the $Z(3)$ walls necessarily requires such CP violating interaction which needs the extraction of A_0 condensate from the $l(x)$ profile. Thus we considered the quark interaction with the wall modeled in terms of an effective $l(x)$ dependent quark mass. Again using the space dependent mass as perturbation and using first order time-dependent perturbation theory we found that quarkonia on interaction with $Z(3)$ walls has non-zero probability of getting excited to higher states, which are short lived in the medium. Here we have only spatial excitation. In this case the transition probability first increases with velocity, attains a maximum value, and subsequently decreases.

In the last work we showed that not only due to $Z(3)$ walls in the medium, during thermalization also quarkonia can get excited because of the time dependence of the potential between quark and antiquark. In the conventional mechanism of quarkonia suppression due to Debye screening, an essential assumption is that when quark-antiquark potential changes in the medium, the quarkonia wave function modifies itself adiabatically to remain in the instantaneous eigen state of the Hamiltonian. Thus, no transitions to other states are considered during the evolution of the potential. Such an assumption of adiabaticity requires that the time scale for potential change should be much larger compared to the dynamical time scale of the quarkonia, e.g. the time scale associated with transition rate between various energy states. At very high energies in RHICE, it is likely that thermalization is achieved in a very short time which is comparable to, or even smaller than, the time scale of transition between quarkonia states. This implies that the validity of adiabatic evolution does not hold and the problem needs to be treated using time dependent perturbation theory. One should then calculate the survival probability of quarkonia during the change of the potential. Considering the thermalization time scale to be small enough (from various estimates and elliptic flow data) we have used sudden approximation. We found that even when temperature of QGP remains below T_D, the quarkonium

state decays with significant probability. This probability increases with temperature of the medium. We have also estimated the error in using this sudden approximation and found that the error remains below 8 % for the thermalization time of about 0.5 fm.

Bibliography

[1] E. M. Riordan, Science **256**, 1287 (1992).

[2] J. Friedman, In *Stanford 1992, The rise of the standard model* 566-588

[3] M. E. Peskin and D. V. Schroeder, Reading, USA: Addison-Wesley (1995) 842 p

[4] L. H. Ryder, Cambridge, Uk: Univ. Pr. (1985) 443p

[5] A. Lahiri and P. B. Pal, Harrow, UK: Alpha Sci. Int. (2005) 380 p

[6] D. J. Gross and F. Wilczek, Phys. Rev. Lett. **30**, 1343 (1973).

[7] H. D. Politzer, Phys. Rev. Lett. **30**, 1346 (1973).

[8] K. Johnson, Acta Phys. Polon. B **6**, 865 (1975).

[9] C. Y. Wong, Singapore, Singapore: World Scientific (1994) 516 p

[10] F. E. Close, Academic Press/london 1979, 481p

[11] U. Reinosa, J. Serreau, M. Tissier and N. Wschebor, Phys. Lett. B **742**, 61 (2015) [arXiv:1407.6469 [hep-ph]].

[12] J. Cleymans, R. V. Gavai and E. Suhonen, Phys. Rept. **130**, 217 (1986).

[13] K. Fukushima and T. Hatsuda, Rept. Prog. Phys. **74**, 014001 (2011) [arXiv:1005.4814 [hep-ph]].

[14] Y. Aoki, G. Endrodi, Z. Fodor, S. D. Katz and K. K. Szabo, Nature **443**, 675 (2006) [hep-lat/0611014].

[15] C. DeTar and U. M. Heller, Eur. Phys. J. A **41**, 405 (2009) [arXiv:0905.2949 [hep-lat]].

[16] K. Rajagopal and F. Wilczek, In *Shifman, M. (ed.): At the frontier of particle physics, vol. 3* 2061-2151 [hep-ph/0011333].

[17] N. D. Mermin, Rev. Mod. Phys. **51**, 591 (1979).

[18] T. W. B. Kibble, J. Phys. A **9**, 1387 (1976).

[19] L. D. McLerran and B. Svetitsky, Phys. Rev. D **24**, 450 (1981).

[20] R. D. Pisarski, Phys. Rev. D **62**, 111501 (2000) [hep-ph/0006205].

[21] R. D. Pisarski, hep-ph/0203271.

[22] A. Dumitru and R. D. Pisarski, Phys. Lett. B **504**, 282 (2001) [hep-ph/0010083].

[23] A. Dumitru and R. D. Pisarski, Nucl. Phys. A **698**, 444 (2002) [hep-ph/0102020].

[24] A. Dumitru and R. D. Pisarski, Phys. Rev. D **66**, 096003 (2002) [hep-ph/0204223].

[25] G. Boyd, J. Engels, F. Karsch, E. Laermann, C. Legeland, M. Lutgemeier and B. Petersson, Nucl. Phys. B **469**, 419 (1996) [hep-lat/9602007].

[26] M. Okamoto *et al.* [CP-PACS Collaboration], Phys. Rev. D **60**, 094510 (1999) [hep-lat/9905005].

[27] B. Layek, A. P. Mishra and A. M. Srivastava, Phys. Rev. D **71**, 074015 (2005) [hep-ph/0502250].

[28] U. S. Gupta, R. K. Mohapatra, A. M. Srivastava and V. K. Tiwari, Phys. Rev. D **82**, 074020 (2010) [arXiv:1007.5001 [hep-ph]].

[29] U. S. Gupta, R. K. Mohapatra, A. M. Srivastava and V. K. Tiwari, Indian J. Phys. **85**, 115 (2011).

[30] A. Atreya, A. M. Srivastava and A. Sarkar, Phys. Rev. D **85**, 014009 (2012) [arXiv:1111.3027 [hep-ph]].

[31] D. M. Elliott and D. H. Rischke, Nucl. Phys. A **671**, 583 (2000) [nucl-th/9908004].

[32] B. I. Abelev *et al.* [STAR Collaboration], Phys. Rev. C **77**, 054901 (2008) [arXiv:0801.3466 [nucl-ex]].

[33] T. Peitzmann, Pramana **60**, 651 (2003) [nucl-ex/0201003].

[34] G. Agakichiev *et al.* [CERES Collaboration], Phys. Rev. Lett. **75**, 1272 (1995).

[35] A. Toia [PHENIX Collaboration], Nucl. Phys. A **774**, 743 (2006) [nucl-ex/0510006].

[36] S. Nagamiya, Nucl. Phys. A **544**, 5C (1992).

[37] F. Antinori *et al.* [NA57 Collaboration], J. Phys. G **32**, 427 (2006) [nucl-ex/0601021].

[38] B. I. Abelev *et al.* [STAR Collaboration], Phys. Rev. C **77**, 044908 (2008) [arXiv:0705.2511 [nucl-ex]].

[39] A. R. Timmins [STAR Collaboration], J. Phys. G **36**, 064006 (2009) [arXiv:0812.4080 [nucl-ex]].

[40] J. Rafelski and B. Muller, Phys. Rev. Lett. **48**, 1066 (1982) [Erratum-ibid. **56**, 2334 (1986)].

[41] P. Koch, B. Muller and J. Rafelski, Phys. Rept. **142**, 167 (1986).

[42] K. H. Ackermann *et al.* [STAR Collaboration], Phys. Rev. Lett. **86**, 402 (2001) [nucl-ex/0009011].

[43] P. F. Kolb and U. W. Heinz, In *Hwa, R.C. (ed.) et al.: Quark gluon plasma* 634-714 [nucl-th/0305084].

[44] P. Romatschke and U. Romatschke, Phys. Rev. Lett. **99**, 172301 (2007) [arXiv:0706.1522 [nucl-th]].

[45] D. A. Teaney, arXiv:0905.2433 [nucl-th].

[46] R. Chatterjee, E. S. Frodermann, U. W. Heinz and D. K. Srivastava, Phys. Rev. Lett. **96**, 202302 (2006) [nucl-th/0511079].

[47] A. Adare *et al.* [PHENIX Collaboration], Phys. Rev. Lett. **109**, 122302 (2012) [arXiv:1105.4126 [nucl-ex]].

[48] O. Linnyk, V. P. Konchakovski, W. Cassing and E. L. Bratkovskaya, Phys. Rev. C **88**, 034904 (2013) [arXiv:1304.7030 [nucl-th]].

[49] O. Linnyk, W. Cassing and E. L. Bratkovskaya, Phys. Rev. C **89**, no. 3, 034908 (2014) [arXiv:1311.0279 [nucl-th]].

[50] K. Adcox *et al.* [PHENIX Collaboration], Phys. Rev. Lett. **88**, 022301 (2002) [nucl-ex/0109003].

[51] C. Adler *et al.* [STAR Collaboration], Phys. Rev. Lett. **89**, 202301 (2002) [nucl-ex/0206011].

[52] G. Aad *et al.* [ATLAS Collaboration], Phys. Rev. Lett. **105**, 252303 (2010) [arXiv:1011.6182 [hep-ex]].

[53] H. Satz, Nucl. Phys. A **418**, 447C (1984).

[54] T. Matsui and H. Satz, Phys. Lett. B **178**, 416 (1986).

[55] M. C. Abreu *et al.* [NA50 Collaboration], Phys. Lett. B **410**, 337 (1997).

[56] B. Alessandro *et al.* [NA50 Collaboration], Eur. Phys. J. C **39**, 335 (2005) [hep-ex/0412036].

[57] E. Eichten, K. Gottfried, T. Kinoshita, K. D. Lane and T. M. Yan, Phys. Rev. D **21**, 203 (1980).

[58] C. Quigg and J. L. Rosner, Phys. Rept. **56**, 167 (1979).

[59] F. Karsch, M. T. Mehr and H. Satz, Z. Phys. C **37**, 617 (1988).

[60] D. J. Gross, R. D. Pisarski and L. G. Yaffe, Rev. Mod. Phys. **53**, 43 (1981).

[61] A. Adare *et al.* [PHENIX Collaboration], Phys. Rev. Lett. **98**, 232301 (2007) [nucl-ex/0611020].

[62] A. Adare *et al.* [PHENIX Collaboration], Phys. Rev. C **84**, 054912 (2011) [arXiv:1103.6269 [nucl-ex]].

[63] B. Abelev *et al.* [ALICE Collaboration], Phys. Rev. Lett. **109**, 072301 (2012) [arXiv:1202.1383 [hep-ex]].

[64] B. B. Abelev *et al.* [ALICE Collaboration], Phys. Lett. B **738**, 361 (2014) [arXiv:1405.4493 [nucl-ex]].

[65] L. D. Landau, E. M. Lifshitz, (1977). Quantum Mechanics: Non-Relativistic Theory. Vol. 3 (3rd ed.). Pergamon Press.

[66] Y. Aharonov and J. Anandan, Phys. Rev. Lett. **58**, 1593 (1987).

[67] A. P. Mishra, A. M. Srivastava and V. K. Tiwari, Indian J. Phys. **85**, 1161 (2011).

[68] C. P. Korthals Altes and N. J. Watson, Phys. Rev. Lett. **75**, 2799 (1995) [hep-ph/9411304].

[69] C. P. Korthals Altes, K. M. Lee and R. D. Pisarski, Phys. Rev. Lett. **73**, 1754 (1994) [hep-ph/9406264].

[70] C. P. Korthals Altes, In *Dallas 1992, Proceedings, High energy physics, vol. 2* 1443-1447

[71] A. Atreya, P. Bagchi and A. M. Srivastava, Phys. Rev. C **90**, no. 3, 034912 (2014) [arXiv:1404.5697 [hep-ph]].

[72] H. Satz, J. Phys. G **32**, R25 (2006) [hep-ph/0512217].

[73] F. Giannuzzi and M. Mannarelli, Phys. Rev. D **80**, 054004 (2009) [arXiv:0907.1041 [hep-ph]].

[74] G. Lacroix, C. Semay, D. Cabrera and F. Buisseret, Phys. Rev. D **87**, no. 5, 054025 (2013) [arXiv:1210.1716 [hep-ph]].

[75] G. S. Bali, Phys. Rev. D **62**, 114503 (2000) [hep-lat/0006022].

[76] A. Nakamura and T. Saito, Phys. Lett. B **621**, 171 (2005) [hep-lat/0512043].

[77] Y. Nakagawa, A. Nakamura, T. Saito and H. Toki, Phys. Rev. D **77**, 034015 (2008) [arXiv:0802.0239 [hep-lat]].

[78] S. Digal, O. Kaczmarek, F. Karsch and H. Satz, Eur. Phys. J. C **43**, 71 (2005) [hep-ph/0505193].

[79] B. Layek, A. P. Mishra, A. M. Srivastava and V. K. Tiwari, Phys. Rev. D **73**, 103514 (2006) [hep-ph/0512367].

[80] S. C. Phatak, Phys. Rev. C **58**, 2383 (1998) [nucl-th/9805009].

[81] P. Bagchi and A. M. Srivastava, Mod. Phys. Lett. A **30**, 32, 1550162 (2015) [arXiv:1411.5596 [hep-ph]].

[82] P. M. Chesler and W. van der Schee, Int. J. Mod. Phys. E **24**, 10, 1530011 (2015) [arXiv:1501.04952 [nucl-th]].

[83] F. Gelis, Int. J. Mod. Phys. E **24**, 10, 1530008 (2015) [arXiv:1508.07974 [hep-ph]].

[84] A. El, Z. Xu and C. Greiner, Nucl. Phys. A **806**, 287 (2008) [arXiv:0712.3734 [hep-ph]].

[85] N. Dutta and N. Borghini, arXiv:1206.2149 [nucl-th].

[86] N. Dutta, A. K. Chaudhuri and P. K. Panigrahi, arXiv:1311.2875 [nucl-th].

[87] J. I. Kapusta and A. Mocsy, Phys. Rev. C **59**, 2937 (1999) [nucl-th/9812013].